View metadata, citation and similar papers at core.ac.uk

brought to you by CORE

provided by NASA Technical Reports Server

NASA-CR-190736

IN-08-CR
117785
p- 50

Computational Aspects of Helicopter Trim Analysis and Damping Levels from Floquet Theory

Final Technical Report Under NASA-Ames Research Grant No. NAG 2-727
(August 1, 1991 - July 31, 1992)

By G. H. Gaonkar
N. S. Achar

Prepared for the Aeroflightdynamics Directorate

U. S. Army Aviation Research and Technology Activity

Ames Research Center

Moffett Field, CA 943035

FLORIDA ATLANTIC UNIVERSITY
Department of Mechanical Engineering
School of Engineering
Boca Raton, FL 33431

September, 1992

(NASA-CR-190736) COMPUTATIONAL ASPECTS OF HELICOPTER TRIM ANALYSIS AND DAMPING LEVELS FROM FLOQUET THEORY Final Technical Report, 1 Aug. 1991 - 31 Jul. 1992 (Florida Atlantic Univ.) 50 p

N92-33107

Unclas

G3/08 0117785

Scope of NASA-Ames Research Grant No. NAG 2-727

Work under this agreement started on August 1, 1991. This final report is presented in two parts. The first part refers to computing the helicopter trim settings of periodic initial states and control inputs sequentially and in parallel. The second part refers to an exploratory study of a subspace iteration method as an alternative to the QR method for Floquet eigenanalysis. The papers resulting from this study are:

1) Achar, N. S., and Gaonkar, G. H., "Helicopter Trim Analysis by Shooting and Finite Element Methods with Optimally Damped Newton Iterations", (In press) *American Institute of Aeronautics and Astronautics Journal,* 1993.

2) Achar, N. S., and Gaonkar, G. H., "An Exploratory Study of a Subspace Iteration Method as an Alternative to the QR Method for Floquet Eigenanalysis", submitted for possible publication in the *Journal of American Helicopter Society.*

PART - I

TRIM ANALYSIS

G. H. Gaonkar
N. S. Achar

Helicopter Trim Analysis by Shooting and Finite Element Methods with Optimally Damped Newton Iterations

Abstract

Helicopter trim settings of periodic initial state and control inputs are investigated for convergence of Newton iteration in computing the settings sequentially and in parallel. The trim analysis uses a shooting method and a weak version of two temporal finite element methods with displacement formulation and with mixed formulation of displacements and momenta. These three methods broadly represent two main approaches of trim analysis: adaptation of initial-value and finite element boundary-value codes to periodic boundary conditions, particularly for unstable and marginally stable systems. In each method, both the sequential and in-parallel schemes are used and the resulting nonlinear algebraic equations are solved by damped Newton iteration with an optimally selected damping parameter. The impact of damped Newton iteration, including earlier-observed divergence problems in trim analysis, is demonstrated by the maximum condition number of the Jacobian matrices of the iterative scheme and by virtual elimination of divergence. The advantages of the in-parallel scheme over the conventional sequential scheme are also demonstrated.

Notation

a	=Lift curve slope
c	=Control-input vector
C_d	=Resultant profile drag force in the plane of the rotor disk opposite to the flight direction
C_{d0}	=Profile drag coefficient

C_l =Rolling moment coefficient

C_m =Pitching moment coefficient

C_t =Thrust coefficient

C_φ =Blade pitching-moment coefficient

C_w =Weight coefficient of the helicopter

$\bar{f}$ =Equivalent flat plate area of parasite drag

F_β, F_ζ =Aerodynamic moment per unit length of the blade in flap and lag directions, respectively

$g(\mathbf{s})$ =Objective function to be minimized

H =Hamiltonian

$[I]$ =Identity matrix

J =Jacobian or nondimensional torsional inertia

L =Lagrangian

p =Generalized momentum ($L_{\dot{q}}$)

P_β =Flap natural frequency (rotating)

q =Generalized coordinate

Q =Nonconservative force

R =Rotor radius

$\mathbf{s}$ =State vector $\mathbf{y}$ augmented with control-input vector $\mathbf{c}$

t_o, t_f =Initial and final times

T =Kinetic energy

V =Flight speed or Potential energy

W =Work done by Q

$\mathbf{y}$ =State vector

$\mathbf{y}(t;\mathbf{y}_0)$ =$\mathbf{y}(t)$ with initial condition $\mathbf{y}(0) = \mathbf{y}_0$

α_s =Shaft tilt angle

β =Flap response

ζ =Lag response

ψ =Azimuth angle

$\theta_0, \theta_c, \theta_s$ =Collective, longitudinal cyclic and lateral cyclic pitch angles, respectively

θ =Pitch angle ($= \theta_0 + \theta_c \cos\psi + \theta_s \sin\psi$)

μ =Advance ratio ($= V \cos\alpha_s / \Omega R$)

$\bar{\mu}$ =Dimensionless flight speed ($= V/\Omega R$)

$\omega_\beta, \omega_\zeta, \omega_\varphi$ =Dimensionless nonrotating flap, lag and torsional natural frequencies

Ω =Rotor speed

γ =Lock number (blade inertia parameter)

λ =Newton damping parameter

λ_i =Inflow

ξ =Newton direction (see Eqs. 4 and 5)

σ =Rotor solidity

$[]^t$ =Transpose of []

$\|\cdot\|$ =Vector norm

∇g =Gradient of g

$(\dot{})$ =Time derivative of ( )

$(\,)_q$ =Partial derivative of ( ) w.r.t. q, similarly subscripts p, q, $\dot{q}$, c and y indicate partial differentiation.

Introduction

The helicopter trim settings comprise control inputs for required flight conditions and the corresponding initial conditions for periodic response. They are prerequisite for stability and vibration studies. The control inputs are specified indirectly so as to satisfy flight conditions of prescribed thrust levels, rolling and pitching moments etc. In addition to the

nonlinearity of the system and control-input equations, the control inputs appear not only in the system damping and stiffness matrices but in the input matrix as well, and must be found concomitantly with the periodic response. The prediction of trim settings has been vigorously pursued since the 1980s and still is a demanding exercise because of divergence of iterative schemes and excessive machine time (Refs. 1–6).

Particularly, for marginally stable and unstable systems, the shooting method is increasingly used (e.g., 2GCHAS, Ref. 7); however, much recent research has been centered on temporal finite element methods of different versions, such as displacement, mixed and bilinear formulations, with further classifications in each of these formulations involving h, p and hp versions (Refs. 4,5,8,9). No matter which method is used, computation of trim settings leads to nonlinear algebraic and transcendental equations, whose solution at present cannot be based on solid theory (Ref. 10). In fact, the computational difficulties of these equations virtually preclude the translation of several trim analysis methods into robust algorithms with global or reasonably qualified convergence characteristics. Little information is available on the nature of such difficulties or on ways to quantify and alleviate them. Newton's method is the most widely used and perhaps the best method of solving nonlinear equations (Ref. 10). But while it guarantees quadratic convergence (the number of significant or accurate digits doubles after each iteration), it guarantees only local convergence and is sensitive to the initial guesses or starting values. And even with good starting values, the method can exhibit erratic divergence due to numerical corruption (Ref. 1).

The present investigation covers this divergence problem with respect to the shooting and two temporal finite element methods, which typify broadly two classes of methods: adaptation of time marching methods of initial-value problems and finite element methods of boundary-value problems to periodic boundary conditions. It also covers the in-parallel scheme or the simultaneous computation of initial conditions and control inputs vis-a-vis the sequential scheme (Ref. 2), in which the iterations for the initial conditions and control

inputs are carried out as two separate computational blocks, one following the other (Refs. 1,2). It must be emphasized that the divergence problem is not peculiar to the in-parallel scheme. In fact it is as much a part of the sequential scheme. Moreover, the bulk of the earlier trim analysis investigation uses sequential computation. An exception is Ref. 1, which found appreciable machine time saving through the in-parallel scheme in the shooting method. However, that finding is masked by erratic divergence of Newton iteration.

Given this background, the present investigation is noteworthy in the following respects:

1. The Newton damping parameter is examined concerning both its selection (with a rational basis of minimizing an objective function) and its role in alleviating the sensitivity of Newton iteration to the starting values in the solution of trim settings of initial state and control inputs.

2. The computational reliability of the Newton iteration without and with optimal damping is quantified by the condition number of the Jacobian matrix, which also explains rationally the earlier-observed divergence problems (Ref. 1).

3. Concerning divergence and machine time, a comprehensive comparison of the sequential and in-parallel schemes is provided; each scheme is treated with Newton iteration both without and with damping. This exercise includes three trim analysis methods, representing two main approaches of trim analysis, particularly in stability investigations.

Damped Newton method

The method retains the highly attractive features of the original Newton method (e.g., quadratic convergence) and yet almost global convergence (Ref. 10). We consider the solution of n nonlinear equations

$$f_i(s_1,s_2, \ldots,s_n) = 0; \quad i = 1,2,\ldots,n \tag{1}$$

or, in equivalent form,

$$f(s) = 0 \tag{2}$$

for which the Jacobian matrix is given by

$$J(s) = \frac{\partial f}{\partial s} = \frac{\partial f_i}{\partial s_j} ; i,j = 1,2, \ldots,n \tag{3}$$

The algorithm begins with the "improved" solution

$$s^{m+1} = s^m + \lambda\xi \tag{4}$$

where m is the iteration counter, λ is the "optimal" damping factor and ξ is the solution of the linear system,

$$\xi = - J(s)^{-1} f(s) \tag{5}$$

The terms *improved* and *optimal* are qualified in the absence of a solution s^* such that $f(s^*) = 0$ and of optimality conditions to determine λ. The theory of unconstrained minimization and weak line search (Refs. 10,11) provides a rational basis of quantifying these two terms and solving for the damping factor. We bypass the mathematical details and include instead a brief account of the method, following Ascher et al. (Ref. 10).

s^{m+1} is an improvement over s^m in the sense of minimizing an associated objective function $g(s^m + \lambda\xi)$ monotonically, where

$$g(s) = 0.5 \sum_{i=1}^{n} f_i(s)^2 \tag{6}$$

The objective function has the property that $g(s) > 0$ and $g(s^*) = 0$ when $f(s^*) = 0$. Thus, the minimum of g(s) provides the solution. Moreover, the Newton direction is a descent direction; that is, for the gradient ∇g, we have

$$\xi^t \nabla g = - [J^{-1} f]^t [J^t f] \tag{7a}$$

$$= - f(s)^2 = -2g < 0 \tag{7b}$$

Expanding $g(s+\lambda\xi)$, we obtain

$$g(s^m + \lambda\xi) = g(s^m) + \lambda\xi^t \nabla g(s^m) + O(\lambda^2 \, |\xi|^2) \; < g(s^m) \tag{8}$$

where ∇g, which is equal to $J^t f$, shows that minimization is sought in the Newton's direction. Thus s^{m+1} is an improvement over s^m in the sense that

$$g(s^{m+1}) = g(s^m + \lambda\xi) < g(s^m) \tag{9}$$

which says that the solution s^* is keyed to the generation of monotonically decreasing values of $g(s)$.

We define from Eq. (8)

$$\varphi(\lambda) = \frac{g(s^m + \lambda\xi) - g(s^m)}{\lambda\, \xi^t \nabla g(s^m)} \tag{10}$$

The algorithm (Refs. 10,11) makes use of a fixed parameter σ such that

$$0 < \sigma < 0.5 \tag{11a}$$

$$\sigma \leq \varphi(\lambda) \leq (1-\sigma) \tag{11b}$$

From Eqs. (8) and (11), we have

$$(1-2\lambda\,(1-\sigma))\, g(s^m) \leq g(s^{m+1}) \leq (1-2\lambda\sigma)\, g(s^m) \tag{12}$$

The role of σ is sketched in Fig. 1, which shows the inherent predictor-corrector structure of the algorithm (Ref. 10). For the mth iteration counter, we approximate the scalar objective function by a quadratic:

$$g(s^m + \lambda\xi) \approx a\lambda^2 + b\lambda + c = \psi(\lambda) \tag{13}$$

where the three unknown constants — a,b and c — are determined from the following conditions:

$$\psi(0) = g(s^m) \tag{14a}$$

$$\psi(\lambda_m) = g(s^m + \lambda_m\xi) \tag{14b}$$

$$\psi'(0) = \frac{d}{d\lambda}\,(\, s^m + \lambda\xi)\Big|_{\lambda\,=\,0} = \xi^t \nabla g(s^m) \tag{14c}$$

The criterion that $\psi(\lambda)$ is a minimum with respect to λ can be expressed as

$$\lambda = \frac{-\lambda_m^2\ \psi'(0)}{2(\psi(\lambda_m) - \psi(0) - \lambda_m\psi'(0))} \leq \frac{\lambda_m}{2(1-\sigma)} \tag{15}$$

The preceding algorithm has been found to work generally well (Ref. 10); direct computational experience in computing trim settings supports this as well. However, there are cases of the algorithm breaking down when the objective function fails to decrease monotonically. That is, when g(s) has local minima and/or singularities, Eq. (13) may not be a good approximation to g(s). Hence, the algorithm fails to compute λ satisfying Eq. (9). This problem has been alleviated as follows. At the end of every iteration, before

computing the damping parameter λ, $\mathbf{s}^{m+1} = \mathbf{s}^m + \lambda\xi$ is computed with $\lambda = 1.0$. Then, if any of the control inputs in $\mathbf{s}^{m+1}$ exceeds physically realistic values (say shaft tilt $\alpha_{s,max} = 20^o$), an upper limit for λ, λ_m, is chosen such that the control inputs in $\mathbf{s}^{m+1}$ are physically realistic. Then, the algorithm proceeds to find optimum λ in the range 0 to λ_m as before. Again, in extreme cases if the algorithm fails to find λ satisfying monotonicity Eq. (9), λ_m itself is chosen as the optimum λ. Though the monotonic decrease in g(s) is not guaranteed with $\lambda = \lambda_m$, the algorithm converges to the trim settings, which are elaborated on later with the help of numerical results.

Condition number of J

The relative error in the solution of trim equations by Newton iteration can be bound by utilization of the condition number of the Jacobian matrix, cond(J), which also quantifies the robustness of the Newton direction; see Eq. (5). To provide an improved appreciation of the role of cond(J), we emphasize that the *actual* computation of trim equations does not follow Eq. (5); it follows a numerically perturbed equation:

$$[J + \delta J]\{\xi + \delta\xi\} = \{f + \delta f\} \tag{16a}$$

The following inequality (Ref. 12)

$$\frac{\|\delta\xi\|}{\|\xi\|} < \text{cond}(J)\left[\frac{\|\delta J\|}{\|J\|} + \frac{\|\delta f\|}{\|f\|}\right] \tag{16b}$$

shows that cond(J) represents the maximum possible magnification of the sum of relative errors in J and **f**. Thus, the higher the value of cond(J), the greater the sensitivity of Eq. (16a) to computational perturbations and, consequently, the less well-conditioned is the computational problem of finding the control inputs and periodic initial state.

With the definition

$$\delta = \max\{\, 1/\text{cond}(J)\,\} \tag{17}$$

and with Eqs. (3) – (7), it can be shown that (Ref. 10)

$$\delta\,|\nabla g|\,|\xi| = \delta|J^t f|\;|J^{-1} f| \le |f|^2 = -\nabla g^t \xi \tag{18}$$

Equations (5) and (18) show that, with increasing value of cond (J), the overall conditioning of the Newton direction decreases. That is, the product $\nabla g^t \xi$ decreases although the correction $|\xi|$ is not small and g(s) does not decrease rapidly along the Newton direction ξ. Schematically stated, lines ab and ac tend to merge with line ad in Fig. 1.

Trim formulation

We include a brief account of the shooting method (Ref. 1) and the weak version of a temporal finite element method with mixed formulation (Ref. 8) of displacements and momenta. The algorithmic details of the temporal finite element method with displacement formulation run similar to those of mixed formulations and are omitted here; for details see Ref. 4. This facilitates appreciation of the algorithmic aspects of sequential and in-parallel schemes of Newton iteration in the trim analysis by the shooting and finite element methods. For convenience, the latter two finite element methods of mixed and displacement versions are, respectively, represented as FEM–M and FEM–D. In the three methods, the algorithm follows the in-parallel scheme or the simultaneous computation of initial conditions and control inputs. The straightforward adaptation to the sequential scheme is not spelled out explicitly.

Shooting method

In trim analysis, equations of motion in state variable form

$$\dot{\mathbf{y}} = \mathbf{G}(\mathbf{y}(t),\mathbf{c}) \tag{21}$$

satisfy the unknown periodic initial state $\mathbf{y}_0$, that is,

$$\mathbf{y}(2\pi;\mathbf{y}_0) - \mathbf{y}_0 = 0 \tag{22}$$

Further, the unknown control inputs $\mathbf{c}$ should be determined such that the desired flight conditions

$$\mathbf{f}(\mathbf{y},\mathbf{c}) = 0 \tag{23}$$

are satisfied. Equations (22) and (23) comprise the nonlinear algebraic trim equations, which are symbolically represented as Eq. (2), where $\mathbf{s} = \lfloor \mathbf{y}, \mathbf{c} \rfloor^t$ is the augmented vector of trim settings. These equations are solved using Newton iteration to get the trim settings.

FEM–M

The Hamilton's Law of Varying Action or HLVA of a system can be represented as

$$\delta \int_{t_0}^{t_f} (L + W)\, dt - (L_{\dot{q}}\, \delta q) \Big|_{t_0}^{t_f} = 0 \tag{24}$$

in which the system is represented in configuration space in terms of the generalized coordinates. In the mixed formulation, we first represent Eq. (24) in terms of the coordinates from the phase space using the Hamiltonian of the system, such that both generalized displacement q and generalized momentum p become primary variables. By varying the Hamiltonian of the system,

$$H = H\,(q,p,t) = p.\dot{q} - L\,(q, \dot{q}, t) \tag{25}$$

we obtain

$$\delta H = \delta p.\dot{q} + p.\delta\dot{q} - \delta L(q,\dot{q},t)$$

Hence,

$$\begin{aligned} \delta L &= \delta p.\dot{q} + p.\delta\dot{q} - \delta H(q,p,t) \\ &= \delta p.\dot{q} + p.\delta\dot{q} - [\, H_q.\delta q + H_p.\delta p \,] \end{aligned}$$

Substituting for δL in Eq. (24), we have

$$\int_{t_0}^{t_f} (\, \delta p.\dot{q} + p.\delta\dot{q} - [\, H_q.\delta q + H_p.\delta p - Q\, \delta q \,]\,)\, dt = (p.\delta q) \Big|_{t_0}^{t_f} \tag{26}$$

In the above equation, $\dot{q}$ occurs only in the first term. Hence, integrating the first term by parts, $\dot{q}$ can be eliminated from the above equation to get

$$\int_{t_0}^{t_f} (\, -\delta\dot{p}.q + p.\delta\dot{q} - [\, H_q.\delta q + H_p.\delta p - Q\, \delta q \,]\,)\, dt = [\, (p.\delta q) - (q.\delta p)] \Big|_{t_0}^{t_f} \tag{27}$$

With the definition

$$\mathbf{y} = \begin{Bmatrix} q \\ p \end{Bmatrix}, \ \delta\mathbf{y} = \begin{Bmatrix} \delta q \\ \delta p \end{Bmatrix}, \ \hat{H} = \begin{Bmatrix} H_q - Q \\ H_p \end{Bmatrix}, \ B = \begin{Bmatrix} p \\ -q \end{Bmatrix}$$

and

$$\begin{Bmatrix} p \\ -q \end{Bmatrix} = \begin{bmatrix} 0 & I \\ -I & 0 \end{bmatrix} \begin{Bmatrix} q \\ p \end{Bmatrix} = \hat{N}.\mathbf{y} \tag{28}$$

Eq. (27) can be expressed in vectorial form:

$$\int_{t_0}^{t_f} (\delta\dot{\mathbf{y}}.\hat{N}\mathbf{y} - \delta\mathbf{y}.\hat{H}) \, dt = [\delta\mathbf{y}.B] \Big|_{t_0}^{t_f} \tag{29}$$

When $\hat{H}$, defined in Eq. (28), is nonlinear in $\mathbf{y}$, it can be linearized about a steady state value $\bar{\mathbf{y}}$ as

$$\hat{H} = \hat{H}(\bar{y}) + \hat{H}(\bar{y})_y \, \Delta\mathbf{y} \tag{30}$$

where

$$\hat{H}(\bar{y}) = \begin{Bmatrix} H_q - Q \\ H_p \end{Bmatrix}, \ \hat{H}(\bar{y})_y = \begin{bmatrix} H_{qq} - Q_q & H_{qp} - Q_p \\ H_{pq} & H_{pp} \end{bmatrix} \tag{31}$$

Substituting Eq. (30) in Eq. (29), we obtain

$$\int_{t_0}^{t_f} [\delta\dot{\mathbf{y}}.\hat{N} (\bar{\mathbf{y}} + \Delta\mathbf{y}) - \delta\mathbf{y} \, \hat{H}(\bar{y}) - \delta\mathbf{y} \, [H(\bar{y})_y] \, \Delta\mathbf{y}] \, dt = (\delta\mathbf{y}.B) \Big|_{t_0}^{t_f} \tag{32}$$

Next, the time interval $[t_0,t_f]$ is discretized into m smaller segments; i.e., $t_0 = t_1 < t_2 < ..t_i ..< t_{m+1} = t_f$. In each of these temporal elements, the generalized coordinate q_e and the momentum p_e can be expressed in terms of some appropriate shape functions as follows.

Since the derivatives of q and p do not occur in Eq. (27), constant values with discrete end-momenta and displacements will satisfy the completeness requirements (Ref. 8); i.e., we can have

$$\mathbf{y}_e = \begin{Bmatrix} q \\ p \end{Bmatrix} = \begin{Bmatrix} \bar{q}_i \\ \bar{p}_i \end{Bmatrix} \text{ if } t_i < t < t_{i+1}$$

$$\mathbf{y}_e = \begin{Bmatrix} q_i \\ p_i \end{Bmatrix} \text{ if } t = t_i \; ; \; \mathbf{y}_e = \begin{Bmatrix} q_{i+1} \\ p_{i+1} \end{Bmatrix} \text{ if } t = t_{i+1} \tag{33}$$

However, the virtual displacement and the virtual momentum require piecewise differentiable functions (Ref. 8). Hence, we choose

$$\delta\mathbf{y}_e = \begin{Bmatrix} \delta q \\ \delta p \end{Bmatrix} = \begin{bmatrix} (1-\tau) & 0 & \tau & 0 \\ 0 & (1-\tau) & 0 & \tau \end{bmatrix} \begin{Bmatrix} \delta q_i \\ \delta p_i \\ \delta q_{i+1} \\ \delta p_{i+1} \end{Bmatrix} = M \, \delta\hat{\mathbf{y}}_e \tag{34}$$

with

$$\tau = \frac{(t - t_i)}{(t_{i+1} - t_i)}$$

Substituting for Δy and δy in Eq. (32) from Eqs. (33) and (34), respectively, for the ith time element, we have

$$\delta\hat{\mathbf{y}}_e \left[\int_{t_i}^{t_{i+1}} [\dot{M}^t.\hat{N} \, (\bar{y}_e + \Delta y_e) - M^t \, \hat{H}(\bar{y}) - M^t \, \hat{H}(\bar{y})_y \, \Delta y_e] \, dt - (M^t \, B) \Big|_{t_i}^{t_{i+1}} \right] = 0 \tag{35}$$

Defining

$$F_e = \int_{t_i}^{t_{i+1}} [\, M^t \, \hat{H}(\bar{y}) - \dot{M}^t.\hat{N} \, \bar{y}_e] \, dt, \quad K_e = \int_{t_i}^{t_{i+1}} [M^t \, \hat{H}(\bar{y})_y - \dot{M}^t.\hat{N} \,] \, dt$$

and

$$G_e = (M^t \, B) \Big|_{t_i}^{t_{i+1}} = \begin{Bmatrix} -p_i \\ q_i \\ p_{i+1} \\ -q_{i+1} \end{Bmatrix}$$

Eq. (35) can be expressed as

$$\delta\hat{\mathbf{y}}_e \, [\, F_e + K_e \, \Delta y_e + G_e] = 0 \tag{36}$$

Next, all the m elemental Eqs. (36) are generated and assembled to get the global, linearized variational statement

$$\delta\hat{\mathbf{y}}\,[\,F + K\,\Delta y + G] = 0 \tag{37}$$

where K, F, G, **y**, $\delta\hat{\mathbf{y}}$ are the global stiffness matrix, force vector, momentum vector, displacement vector and the virtual displacement vector, respectively. The elements of the vectors G, **y** and $\delta\hat{\mathbf{y}}$ are given below.

$$G = \lfloor\, -p_1,\, q_1,\, 0,\, \ldots\, 0,\, 0,\, p_{m+1},\, -q_{m+1} \,\rfloor^t \tag{38a}$$

$$\mathbf{y} = \lfloor\, \bar{q}_1,\, \bar{p}_1,\, \bar{q}_2,\, \bar{p}_2, \ldots,\, \bar{q}_m,\, \bar{p}_m \,\rfloor^t \tag{38b}$$

$$\delta\hat{\mathbf{y}} = \lfloor\, \delta q_1,\, \delta p_1,\, \delta q_2,\, \delta p_2 \ldots,\, \delta q_{m+1},\, \delta p_{m+1} \,\rfloor^t \tag{38c}$$

Then, applying the periodic boundary conditions to Eq. (37) (i.e., $q_1 = q_{m+1}$ and $p_1 = p_{m+1}$), we get

$$\mathbf{F} + \mathbf{K}\,\Delta\mathbf{y} = 0 \tag{39}$$

where **F** and **K** are F and K, respectively, rearranged after applying the boundary conditions. Next, Eq. (39) is solved using Newton iteration until the series $\mathbf{y} = \Sigma\,\Delta\mathbf{y}_i$ converges, both **F** and **K** being updated at the end of each iteration.

Parallel trim method

For the parallel solution of trim settings, we reformulate the **F** and **K** of Eq. (39) as follows. Since $\hat{H}$, defined in Eq. (28), is nonlinear in both **y** and **c**, it can be linearized about some mean position $\bar{\mathbf{y}}$ and $\bar{\mathbf{c}}$. (Note: The Hamiltonian H is nonlinear in q and p, and the generalized force Q is nonlinear both in p, q and c.) That is,

$$\hat{H} = [\,\hat{H}(\bar{\mathbf{y}},\bar{\mathbf{c}}) + \hat{H}(\bar{\mathbf{y}},\bar{\mathbf{c}})_y\,\Delta\mathbf{y} + \hat{H}(\bar{\mathbf{y}},\bar{\mathbf{c}})_c\,\Delta\mathbf{c}\,] \tag{40}$$

where

$$\hat{H}(\bar{\mathbf{y}},\bar{\mathbf{c}})_c = \begin{bmatrix} H_{qc} - Q_c \\ H_{pc} \end{bmatrix}$$

and $\hat{H}(\bar{\mathbf{y}},\bar{\mathbf{c}})_y = \hat{H}(\bar{\mathbf{y}})_y$; see Eq. (31). Substituting Eq. (40) in Eq. (29), we get the variational statement for each element as

$$\delta\mathbf{y}_e \Big[\int_{t_i}^{t_{i+1}} [\dot{M}^t.\hat{N}\,(\bar{\mathbf{y}}_e + \Delta\mathbf{y}_e) - M^t\,\hat{H}(\bar{\mathbf{y}}) - M^t\,\hat{H}(\bar{\mathbf{y}})_y\,\Delta\mathbf{y}_e - M^t\hat{H}(\bar{\mathbf{y}},\bar{\mathbf{c}})_c\,\Delta\mathbf{c}]\,dt - (M^t\,B)\Big|_{t_i}^{t_{i+1}} \Big] = 0 \tag{41}$$

Defining

$$F_e = \int_{t_i}^{t_{i+1}} [\, M^t \hat{H}(\bar{y},\dot{c}_y) - \dot{M}^t.\hat{N}\, \bar{y}_e \,]\, dt, \quad K_e = \int_{t_i}^{t_{i+1}} [M^t \hat{H}(\bar{y},\dot{c})_y - \dot{M}^t.\hat{N}\,]\, dt$$

and

$$K_{ec} = \int_{t_i}^{t_{i+1}} [M^t \hat{H}(\bar{y},\dot{c})_c]\, dt, \quad G_e = (M^t B)\Big|_{t_i}^{t_{i+1}} = \begin{Bmatrix} -p_i \\ q_i \\ p_{i+1} \\ -q_{i+1} \end{Bmatrix} \tag{42}$$

Eq. (41) can be represented as

$$\delta\hat{\bar{y}}_e\, [\, F_e + K_e\, \Delta y_e + K_{ec}\, \Delta c + G_e] = 0 \tag{43}$$

Next, all the elemental Eqs. (43) are generated and assembled to get the global, linearized variational statement

$$\delta\hat{\bar{y}}\, [\, F + K\, \Delta y + K_c \Delta c + G] = 0 \tag{44}$$

Further, Eq. (23) can be linearized as

$$f(y,c) = f(\bar{y},\bar{c}) + \left[\, f(\bar{y},\dot{c})_y\, \Delta y + f(\bar{y},\dot{c})_c\, \Delta c \,\right] = 0 \tag{45}$$

Now, Eqs. (44) and (45) are combined and the boundary condition is applied to get the augmented force vector and stiffness matrix, **F** and **K** of Eq. (39), respectively. Then, Eq. (39) is solved iteratively, until the augmented vector $\mathbf{s} = \Sigma\Delta\mathbf{s}_i$ converges where $\Delta\mathbf{s}_i = \lfloor \Delta\mathbf{y}_i, \Delta\mathbf{c}_i \rfloor^t$.

Model description

For computational purposes, flap–lag and flap–lag–torsion models are selected; both the models are based on quasisteady aerodynamics and rigid body mode representation. However, for the simplicity of illustrating the algorithmic and computational aspects, model description and much of the discussion of numerical results are for the flap–lag model, which was also treated in Ref. 1 by the shooting method. We begin with the state vector $\mathbf{y}(t)$ with four components comprising the flap angle β and lag angle ζ and their

rates $\dot{\beta}$ and $\dot{\zeta}$: $\mathbf{y}(t) = \lfloor\, \beta(t),\ \dot{\beta}(t),\ \zeta(t),\ \dot{\zeta}(t)\, \rfloor^t$. Part of the trim analysis is to compute the periodic initial state $\mathbf{y}_0$ such that

$$\mathbf{y}(2\pi;\mathbf{y}_0) - \mathbf{y}_0 = 0 \tag{46}$$

The remaining part of the trim analysis is to compute the four parameters — three pitch angles θ_0, θ_s and θ_c and shaft tilt α_s — to satisfy the following four trim equations of force and moment balance:

$$C_t \cos(\alpha_s) + C_d \sin(\alpha_s) = C_w \tag{47}$$

$$C_t \sin(\alpha_s) - C_d \cos(\alpha_s) = 0.5\, \mu^2\, \bar{f} \tag{48}$$

$$C_l = 0 \tag{49}$$

$$C_m = 0 \tag{50}$$

The solution of four initial-condition equations, typified by Eq. (46) and four trim Eqs.(47) – (50), constitutes the trim analysis. The nondimensional thrust C_t and horizontal force C_d depend on the total blade root shear forces: $\bar{F}_\beta$, normal to the blade in the flap direction; $\bar{F}_\zeta$, in the lag direction, and $\bar{F}_r$, in the outward radial direction. These shear forces are given by

$$\bar{F}_\beta = -1.5\, \ddot{\beta} - 1.5 \cos(\beta) \sin(\beta)(1+\dot{\zeta})^2 + \int_0^1 F_\beta\, dr \tag{51}$$

$$\bar{F}_\zeta = -1.5\, \ddot{\zeta} \cos^2(\beta) + 3 \sin(\beta)\cos(\beta)\, (1+\dot{\zeta})\, \dot{\beta} + \cos\beta \int_0^1 F_\zeta\, dr \tag{52}$$

$$\bar{F}_r = 1.5\, [\, (1+\dot{\zeta})^2 \cos^2(\beta) + \dot{\beta}^2\,] \tag{53}$$

Then, C_t and C_d, in Eqs. (47) – (48), and the rolling moment and the pitching moment coefficients, C_l and C_m, respectively, in Eqs. (49) – (50), are given by

$$\frac{C_t}{\sigma a} = \frac{1}{\gamma\ 2\pi} \int_0^{2\pi} [\bar{F}_\beta \cos(\beta) + \bar{F}_r \cos(\beta)] d\psi \tag{54}$$

$$\frac{C_d}{\sigma a} = \frac{1}{\gamma\ 2\pi} \int_0^{2\pi} [\bar{F}_\beta \sin(\beta)\cos(\psi+\zeta) + \bar{F}_\zeta \sin(\psi+\zeta) + \bar{F}_r \cos(\beta)\cos(\psi+\zeta)]\, d\psi \tag{55}$$

$$\frac{C_l}{\sigma a} = -\frac{(P_\beta^2 - 1)}{\gamma\ 2\pi} \int_0^{2\pi} \beta \sin(\psi+\zeta)\, d\psi \tag{56}$$

$$\frac{C_m}{\sigma a} = -\frac{(P_\beta^2-1)}{\gamma\ 2\pi} \int_0^{2\pi} \beta \cos(\psi+\zeta)\, d\psi \tag{57}$$

The final component of the trim analysis concerns the uniform total inflow λ_i:

$$\lambda_i = \mu \tan(\alpha_s) + C_t/\ [2\sqrt{(\mu^2 + \lambda_i^2)}] \tag{58}$$

which is solved iteratively in combination with C_t and α_s.

Trim analysis results

Trim analysis uses the shooting method and the two finite element methods, FEM–M and FEM–D. The control inputs and initial conditions are computed simultaneously as one block in the in-parallel scheme; they are computed sequentially as two separate blocks in the sequential scheme. Unless stated otherwise, the rigid flap–lag model with in-parallel scheme is used; nonlinear equations are solved by conventional Newton iteration with no damping and the following baseline values are assumed: $\gamma = 5$, $\omega_\beta = 0.57$, $\omega_\zeta = 1.4$, $\sigma = 0.05$, $a = 6.28$, $C_w = 0.01$, $C_{do} = 0.01$, $\bar{f} = 0.01$, $0 \leq \bar{\mu} \leq 0.7$. The computations are performed on a VAX 6320. The sparse matrices obtained by the finite element methods are solved using the NAG subroutine (F01BRF), whcih considers the matrix sparsity.

In the finite element methods, it is first necessary to arrive at the number of elements, NEL, needed for a priori specified level of tolerance in the solution of periodic response. This tolerance is further substantiated on the basis of a relative error norm criterion with the shooting-method results (Refs. 1,2) as reference values. For that purpose, a typical flight speed, $\bar{\mu} = 0.4$ is chosen. As shown in Fig. 2a for a typical initial state $\dot{\beta}(0)$, all the periodic initial conditions, $\mathbf{y} = \lfloor\, \beta(0),\ \dot{\beta}(0),\ \zeta(0),\ \dot{\zeta}(0) \rfloor^t$ converge as the number of elements increases. In particular, it was found that for asymptotic convergence of all the four components of $\mathbf{y}$, we need at least NEL = 12 for FEM–D and NEL = 16 for FEM–M. Concerning the minor differences between results from the three trim methods, the relative error norm in $\mathbf{y} = \lfloor\, \beta,\ \dot{\beta},\ \zeta,\ \dot{\zeta} \rfloor^t$, obtained by the respective FEM, is defined as

$$\text{Relative error norm} = \frac{1}{\text{NEL}} \sqrt{\left[\frac{\Sigma \| y_{shoot} - y_{fem} \|_i^2}{\Sigma \| y_{shoot} \|_i^2} \right]}, \; i = 1,\ldots,\text{NEL}$$

As seen from Fig. 2b, as the number of elements increases, the relative error norm decreases rapidly; for NEL = 12 for FEM–D and for NEL = 16 for FEM–M, the relative error norm is less than 0.01. For the above NEL values selected on the basis of the results at $\bar{\mu} = 0.4$, it was also verified that right up to $\bar{\mu} = 0.7$, the relative error norm is less than 0.01. Thus, in summary, NEL values of 12 and 16 for FEM–D and FEM–M, respectively, guarantee 1) asymptotic convergence for $\bar{\mu} = 0.4$ and 2) a relative error norm of less than 0.01 for $0.0 \leq \bar{\mu} \leq 0.7$. Spot checks for other values of $\bar{\mu}$ show that asymptotic convergence with these NEL values holds for $0.0 \leq \bar{\mu} \leq 0.7$ as well. Overall, with these NEL values, the control inputs θ_0, θ_s, θ_c and α_s, and the periodic responses β, $\dot{\beta}$, ζ and $\dot{\zeta}$, agree with the shooting method results. Hence, these NEL values are chosen in all the subsequent numerical results with the flap-lag model. (This agreement is further elaborated later on for the flap-lag-torsion model.)

In Figs. 3–5, the machine times taken by the sequential and in-parallel schemes in the three trim analysis methods are presented. Given the sensitivity of Newton iteration to starting values, the results for each of the methods are presented for two sets of starting values. In part (a), we use the "exact" solution of the preceding flight speed $\bar{\mu}$ as the starting value; the exact solution is taken as the one obtained by continuation approach with $\bar{\mu}$ as a continuation parameter and $\Delta\bar{\mu} = 0.05$ as the continuation step size. For example, starting values, say at $\bar{\mu} = 0.3$, are given by the solution at the preceding value of $\bar{\mu} = 0.25$. For a given flight speed, the cumulative machine times taken starting from $\bar{\mu} = 0$ are shown in parts (a) of Figs. 3–5. Though prohibitively costly, this approach to the starting values provides a rational basis of providing the 'best' starting values. The other extreme is to begin with zero starting values, perhaps the most demanding starting values for the iteration. This is done in part (b) of Figs. 3–5; owing to the divergence problem of Newton iteration with zero starting values in both the sequential and in-parallel schemes,

the results are limited to $\bar{\mu} \leq 0.3$. Figures 3–5 show that the in-parallel scheme is more economical than the sequential scheme. This saving is observed for both sets of starting values (continuation with $\Delta\bar{\mu} = 0.05$ and zero starting values), showing that the in-parallel scheme is preferable regardless of the starting values.

The preceding results are based on Newton iteration with no damping, and mention is made of the divergence of the iteration with zero starting values. The impact of damped Newton iteration on divergence and related issues are pursued in Figs. 6–9; an important observation is that the damped Newton method did not encounter divergence. Figures 6 and 7 show the mechanism of divergence relative to iteration counter and the starting values. This is followed by Figs. 8 and 9, which show a means of quantifying and understanding divergence as well as computing the Newton damping parameter, which virtually eliminates divergence.

Figure 6 shows the iteration counter versus flight speed. While iteration without damping experiences divergence for approximately $\bar{\mu} = 0.45$, damped iteration does not diverge although its iteration counter increases with increasing $\bar{\mu}$. That the Newton damping parameter makes the iteration more controlled and "gives less room for erratic behavior" (Ref. 10) is well borne out in Fig. 6. Also, for $\bar{\mu} > 0.6$ or so, the iteration counter in the damped iteration rapidly grows in the shooting method, indicating poor convergence. By comparison the damped iteration in FEM–M and FEM–D is remarkably smooth; the iteration counter and its growth with increasing $\bar{\mu}$ are much less rapid and it hardly exceeds 15 for the complete sweep of $0.0 \leq \bar{\mu} \leq 0.7$. As seen from Fig. 6, the FEM–M and FEM–D have fast convergence up to $\bar{\mu} = 0.7$ while the shooting method exhibits slow convergence for $\bar{\mu} \geq 0.65$. Summarizing, we observe that the FEM–M and FEM–D are much better regarding iteration counter or speed of convergence; at $\bar{\mu} = 0.7$ for example, iteration counter for FEM–M and FEM–D is about 15 whereas it is about 55 for the shooting method, nearly four times higher.

The divergence problem of the Newton iteration due to the starting values is further

pursued in Fig. 7 in the $\rho - \bar{\mu}$ plane, where ρ is related to the starting values as

$$\text{starting value} = \rho \text{ x exact solution}$$

Here, $\rho = 0.0$ and $\rho = 1.0$ imply that all the starting values are zero and exact solution, respectively. (The exact solution at any flight speed is that solution obtained by continuation approach with $\Delta\mu = 0.05$). This is done as a means of quantifying the sensitivity to possible extremes of starting values and of connecting these results with an earlier investigation (Ref. 1). The other possibility of large initial values ($\rho > 1$) is not exercised separately. The divergence boundary of Fig. 7 corresponding to the shooting method is similar to that of Ref. 1; the minor differences are due to the sensitivity of these boundaries to discretization in ρ and $\bar{\mu}$. Even with somewhat improved starting values, say $\rho = 0.1$ compared with $\rho = 0.0$, erratic behavior of the boundaries merits mention. The damped Newton iteration reduces the erratic behavior in general; indeed in Fig. 7 it converges everywhere. With poor starting values (low values of ρ, say less than 0.5), divergence with Newton iteration is not unexpected since it guarantees only local convergence and is sensitive to starting values anyway. What is unexpected is divergence in the shooting method for ρ as high as 0.8. Concerning divergence boundary, shooting method is affected more than FEM–M and FEM–D. This supports the iteration counter results in Fig. 6.

The unexpected divergence with Newton iteration and the absence of divergence with damped Newton iteration is further investigated in Fig. 8 on the basis of the maximum condition number of the Jacobian matrices of the iterations; see Eqs. (16a) and (16b), respectively. The results are for $\rho = 0.0$, zero starting values. As seen from Fig. 8, the onset of divergence in Fig. 6 for $\bar{\mu} = 0.50$ in the shooting method and $\bar{\mu} = 0.45$ in FEM–M and FEM–D is accompanied by rapid increase in the Jacobian matrix condition numbers for corresponding values of $\bar{\mu}$. By comparison these condition numbers essentially remain constant in all the three trim analysis methods with damped Newton iteration. This shows that damped Newton iteration significantly improves the overall conditioning of the

iteration.

Figure 9a shows, for $\bar{\mu} = 0.3$, the monotonic decrease of the objective function, see Eq. (6). We emphasize that $g(s) = 0$ gives the damping parameter λ. It is seen that the objective function decay is monotonic on expected lines in all the three trim analysis methods and that the minimization is fairly rapid. That is, the iteration counter hardly exceeding 7 for $g(s) = 10^{-11}$ for each of the three trim analysis methods. Figure 9b shows the initial nonmonotonic decrease of the objective function. In such cases the algorithm follows the remedial measures referred to earlier in conjunction with Eq. (9). Two distinguishing features of Fig. 9b merit mention. First, even in cases when λ cannot be computed on the basis of monotonic decrease of the objective function, the algorithm still converges to the trim settings with as few as 7 iterations in all the three methods. Second, despite a couple of initial iterations involving nonmonotonic decrease, it later, converges with a rapid monotonic decrease.

Thus far, the influence of the damped Newton iteration on the divergence problem of the in-parallel scheme is addressed. We now conclude with a brief discussion of its influence on the sequential scheme. In this scheme, unlike the in-parallel scheme, there are two sets of starting values; one for the response loop and one for the control loop. Without damping, the divergence boundary for the shooting method with the sequential scheme is given in Fig. 10; for the other two methods they remain nearly the same and are not shown. For all the three methods, the starting values for the response loop are assumed zero and those for the control loop are chosen using the starting value parameter ρ:

$$\text{Starting value} = \rho \times \text{exact control settings}$$

where the exact control settings are those obtained by the continuation approach with $\Delta\bar{\mu} = 0.05$. In this scheme, it is observed that the divergence is mainly due to the sensitivity of the response loop to the physically unrealistic values of the control inputs, estimated in the control loop. When the control-input computations are prevented from generating unrealistically large values either by damping or by a priori stipulation, the response is

always found to converge. That is, damping the control loop is more effective than damping the response loop, and, therefore, in this illustrative example, the damped Newton iteration is implemented only in the control loop. After introducing the damped Newton iteration, in both versions of FEM, the sequential scheme converges in the entire $\rho - \bar{\mu}$ plane right up to $\bar{\mu} \leq 0.7$. However, in the shooting method, i.e. Fig. 10, though there is an increase in the region of convergence because of damping the Newton iteration, the iteration was found to cycle for $\bar{\mu}$ beyond 0.55; i.e., after some iterations, the algorithm computes a solution that it has already computed in one of the previous iterations and hence the algorithm enters into an infinite loop without converging. This cycling phenomenon is found to be independent of the ill-conditioning or near-singularity of the Jacobian as quantified by the condition number of the Jacobian. This problem is involved and not well-understood, (Ref. 10) and there seems to be no known method to treat it effectively.

The preceding investigation based on the flap-lag model results is further verified on the basis of flap-lag-torsion model results. The rotor parameters are identical to those of the flap-lag model; the additional torsional parameters are $\omega_\varphi = 3.0$, $J = 0.002$ and $C_\varphi = -0.02$. Overall, the results are nearly identical to those of the flap-lag model results, specifically these results refer to damped Newton iteration (e.g., divergence boundary, condition number and monotonic decrease of objective function) and to sequential scheme vis-a-vis in-parallel scheme. In Fig. 11, we select for illustration the torsional response rate $\dot{\varphi}(t)$ among the six components of the state vector $\mathbf{y} = \lfloor \beta, \dot{\beta}, \zeta, \dot{\zeta}, \varphi, \dot{\varphi} \rfloor^t$ and the shaft-tilt angle α_s among the four components of the control-input vector $\mathbf{c} = \lfloor \theta_0, \theta_c, \theta_s, \alpha_s \rfloor^t$. The results from the three methods agree. Finally, as in Figs. 3–5, Fig. 12 shows the machine time saving with the in-parallel scheme in the FEM–D method; similar trends (not shown) are exhibited by the FEM–M and shooting methods with the in-parallel scheme. The only major difference between the flap-lag and flap-lag-torsion results concern NEL or the number of elements needed for asymptotic convergence of the periodic response as shown in

Fig. 2. For the latter case, because of highly oscillatory nature of the torsional response, NEL values as high as 60 and 90 are needed for FEM–D and FEM–M, respectively (Ref. 14).

Concluding remarks

The three trim analysis methods are investigated with an optimally selected damping parameter λ; $\lambda = 1$ refers to conventional Newton iteration. With each trim analysis method, both the sequential and in-parallel schemes of computations of initial conditions and control inputs are exercised. The computational efficiency is described on the basis of both machine time and convergence characteristics, which are quantified by the maximum condition number of the Jacobian matrices of the Newton iteration. The iteration counter and its growth with increasing flight speed and divergence boundaries correlate with this quantification. That investigation demonstrates the feasibility of using an optimally selected Newton damping parameter in the in-parallel scheme to improve the computational efficiency of the trim analysis. It also shows the following:

1) In the three trim analysis methods with both the sequential and in-parallel schemes, the optimally selected damping parameter virtually eliminates divergence up to flight speed $\bar{\mu} = 0.7$ except for a small region beyond $\bar{\mu} > 0.55$ in shooting method with the sequential scheme.

2) The in-parallel scheme takes much less machine time compared to the sequential scheme with comparable convergence characteristics.

3) At very high advance ratios (for $\bar{\mu} \geq 0.6$ or so), the shooting method shows slow convergence in that the iteration counter and the machine time increase rapidly. By comparison, FEM–M and FEM–D show fast convergence for the entire range of $0 \leq \bar{\mu} \leq 0.7$.

4) The cycling phenomenon observed at $\bar{\mu} > 0.55$ in the shooting method with the

sequential scheme and with damped Newton iteration merits further research.

The preceding investigation is restricted to a generic Newton-Raphson iteration and does not consider a wide class of related methods such as quasi Newton and other globally convergent methods. Nevertheless it should provide a reference point for using and comparatively assessing such methods in helicopter trim analysis.

Acknowledgement

Prof. David A. Peters of Washington University took keen interest during the progress of this investigation and offered several comments. We are grateful to him. This work is partially sponsored by the U.S. Army Research Office under Research Grants DAAL03-87-K-0037 and DAAL03-91-G0007 and the Aeroflightdynamics Directorate of the NASA–Ames Research Center under Research Grant NAG 2-727.

References

1. Peters, D. A. and Izadpanah, A. P., "Helicopter Trim by Periodic Shooting with Newton-Raphson Iteration," Presented at the 37th Annual Forum of the American Helicopter Society, New Orleans, Louisiana, 1981, Paper No. 23.

2. O'Mally III, J. A., Izadpanah, A. P. and Peters, D. A., "Comparison of Three Numerical Trim Methods for Rotor Air Loads," Presented at the Ninth European Rotorcraft Forum, Stresa, Italy, September 1983, Paper No. 58.

3. Izadpanah A. P., *P-Version of Finite Elements for the Space-Time Domain With Application to Floquet Theory*, Ph.D. dissertation, Georgia Institute of Technology, August, 1986, Chapter 3.

4. Borri, M., "Helicopter Rotor Dynamics by Finite Element Time Approximation," *Comp. & Maths. with Appls.*, Vol. 12A, (1), 1986, pp. 149-160.

5. Peters, D. A. and Izadpanah A. P., "hp-version of Finite Elements for the Space–Time Domain," *Computational Mechanics*, Vol. 3, 1988, pp. 73-88.

6. Bauchau, O. A. and Hong, C.H., "Nonlinear Response and Stability Analysis of Beams Using Finite Element in Time," *AIAA Journal*, Vol. 26, (9), 1988, pp. 1135-1142.

7. Stephens, W. B. et. al, "Development of Second Generation Comprehensive Helicopter Analysis System (2GCHAS)," American Helicopter Society National Specialists' Meeting on Rotorcraft Dynamics, Arlington, Texas, November 1989.

8. Hodges, D. H. and Bless, R. B., "A Weak Hamiltonian Finite Element Method for Optimal Control Problems," *Journal of Guidance, Control, and Dynamics*, Vol. 14, 1991, pp. 148-156.

9. Hodges, D. H. and Hou, L. J., "Shape Functions For Mixed p–Version Finite Elements in the Time Domain," *Journal of Sound and Vibration*, Vol. 145, (2), 1991, pp. 169-178.

10. Ascher, U. M., Mattheij, R. M. M. and Russel, R. D., *Numerical Solution of Boundary Value Problems for Ordinary Differential Equations,* Prentice Hall, Inc., Englewood Cliffs, New Jersey, 1988, pp. 327-357.

11. Bertsekas P. D., *Constrained Optimization and Lagrange Multiplier Methods*, Academic Press, New York, 1982, Chapter 1.

12. Ortega, J. M., *Numerical Analysis; A Second Course*, New York, Academic Press, 1972, Chapter 2.

13. Ravichandran, S., Gaonkar, G. H., Nagabhushanam, J. and Reddy T. S. R., "A Study of Symbolic Processing and Computational Aspects in Helicopter Dynamics," *Journal of Sound and Vibration*, Vol. 137, (3), March 1990, 495-507.

14. Achar, N. S., *Trim analysis by Shooting and Finite Elements and Floquet Eigenanalysis by QR and Subspace Iterations in Helicopter Dynamics*, Ph.D. dissertation, Florida Atlantic University, April 1992, Chapter 4.

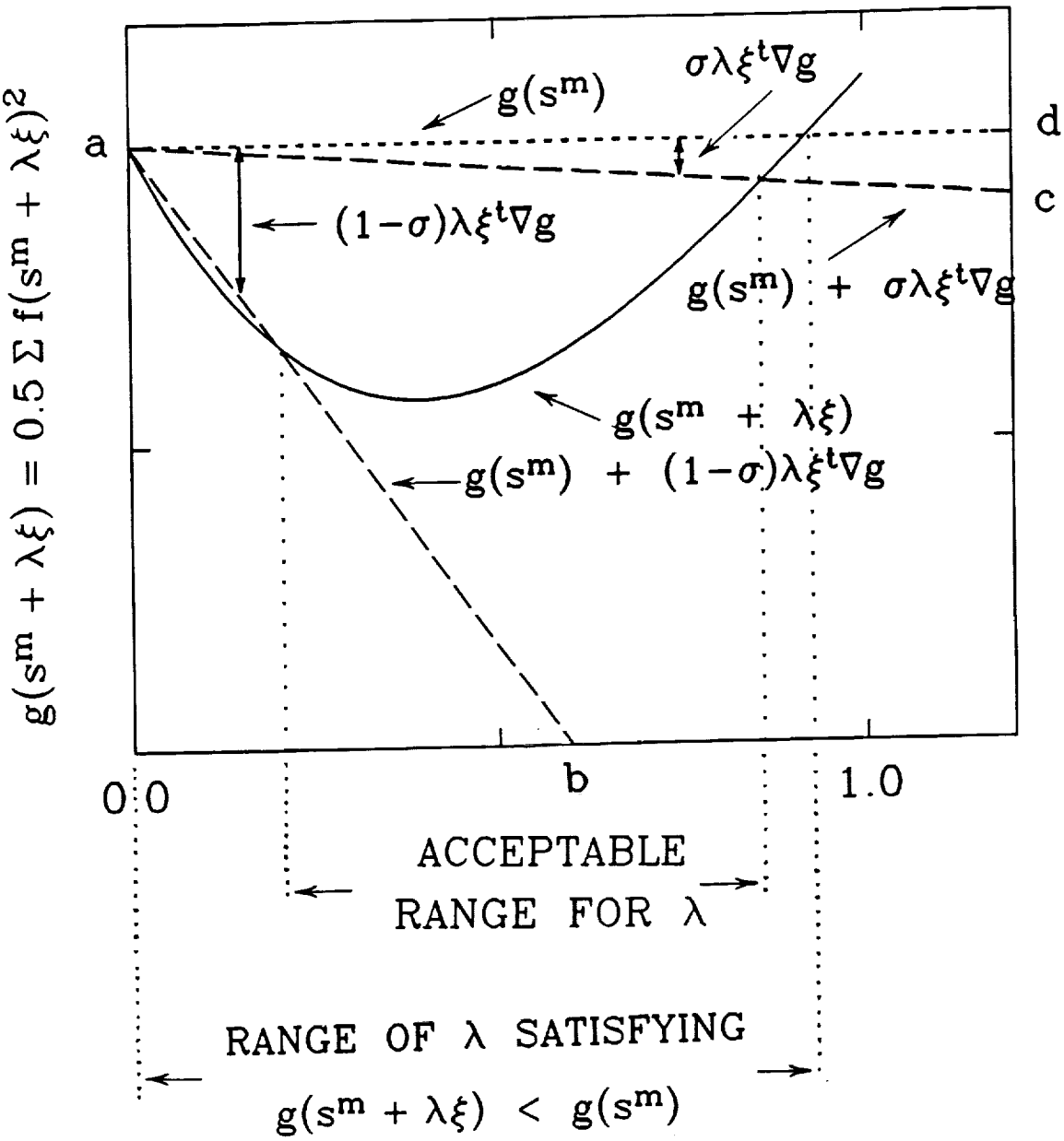

Fig. 1 An acceptable range of the damping parameter λ for the damped Newton iteration

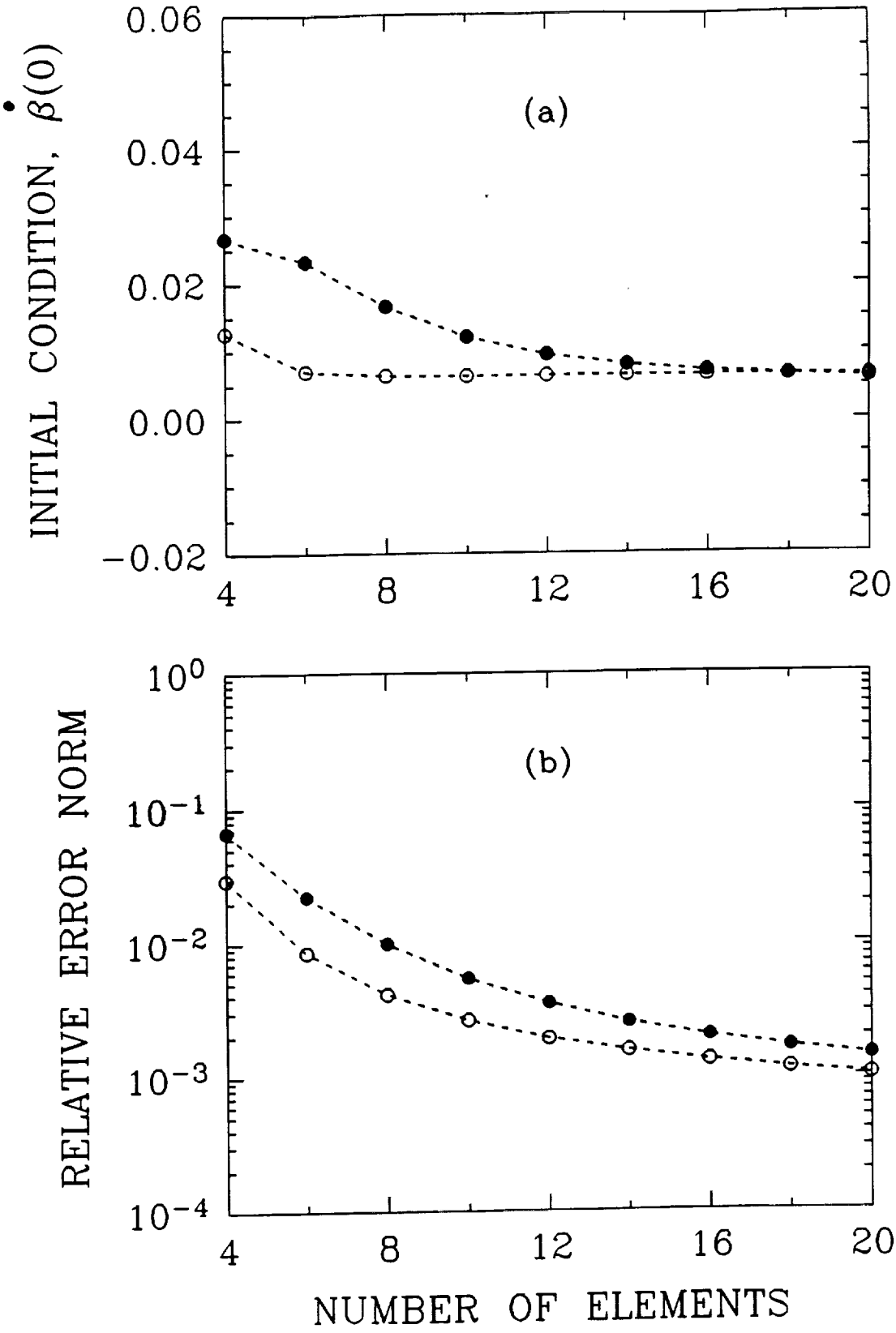

Fig. 2 Convergence of Periodic initial-condition in FEM-D and FEM-M with increasing number of elements at $\bar{\mu}$=0.4 (○·····○ FEM-D, ●·····● FEM-M)

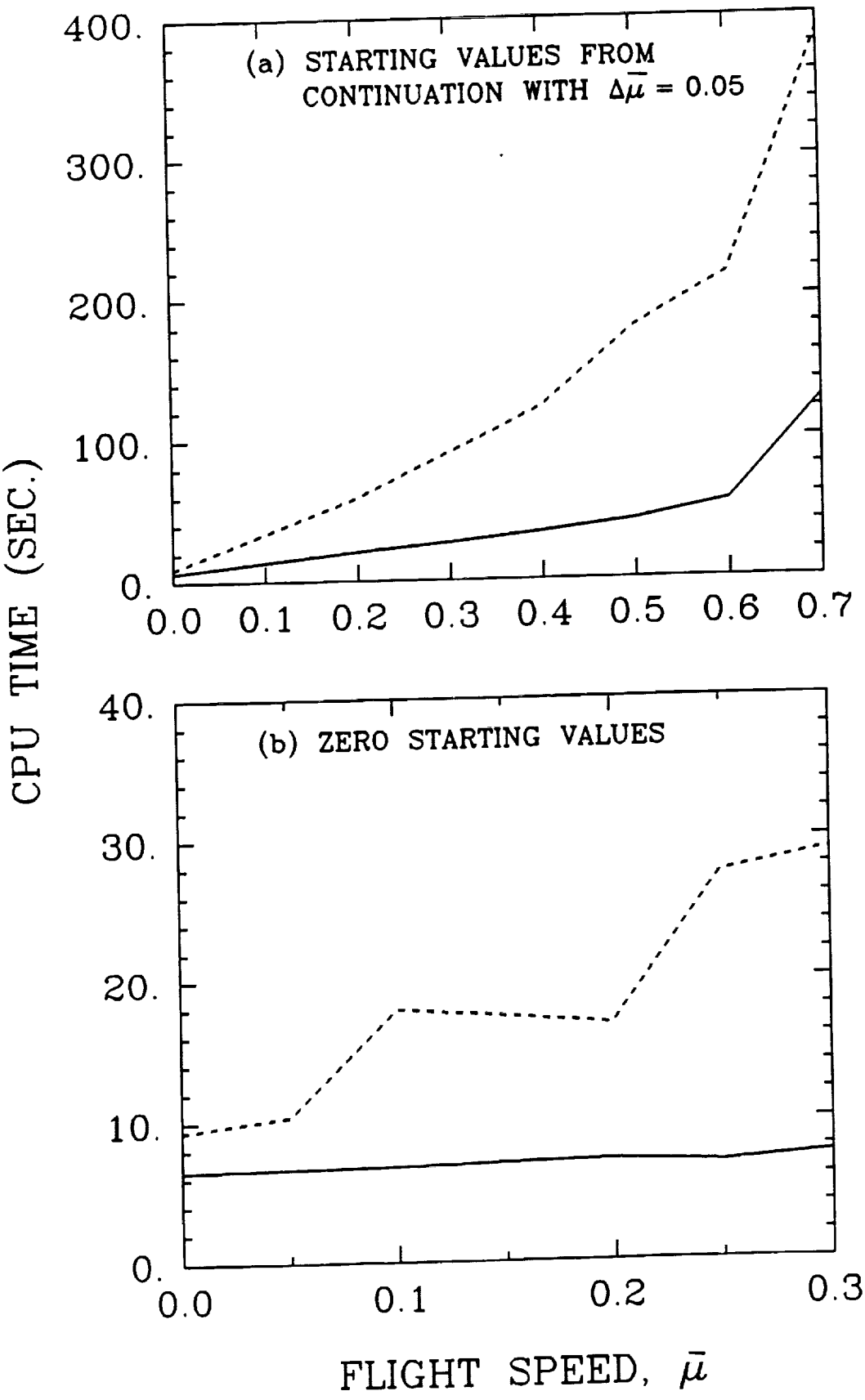

Fig. 3 Machine time comparison in the shooting method with sequential and in-parallel schemes (------- sequential, —— in-parallel)

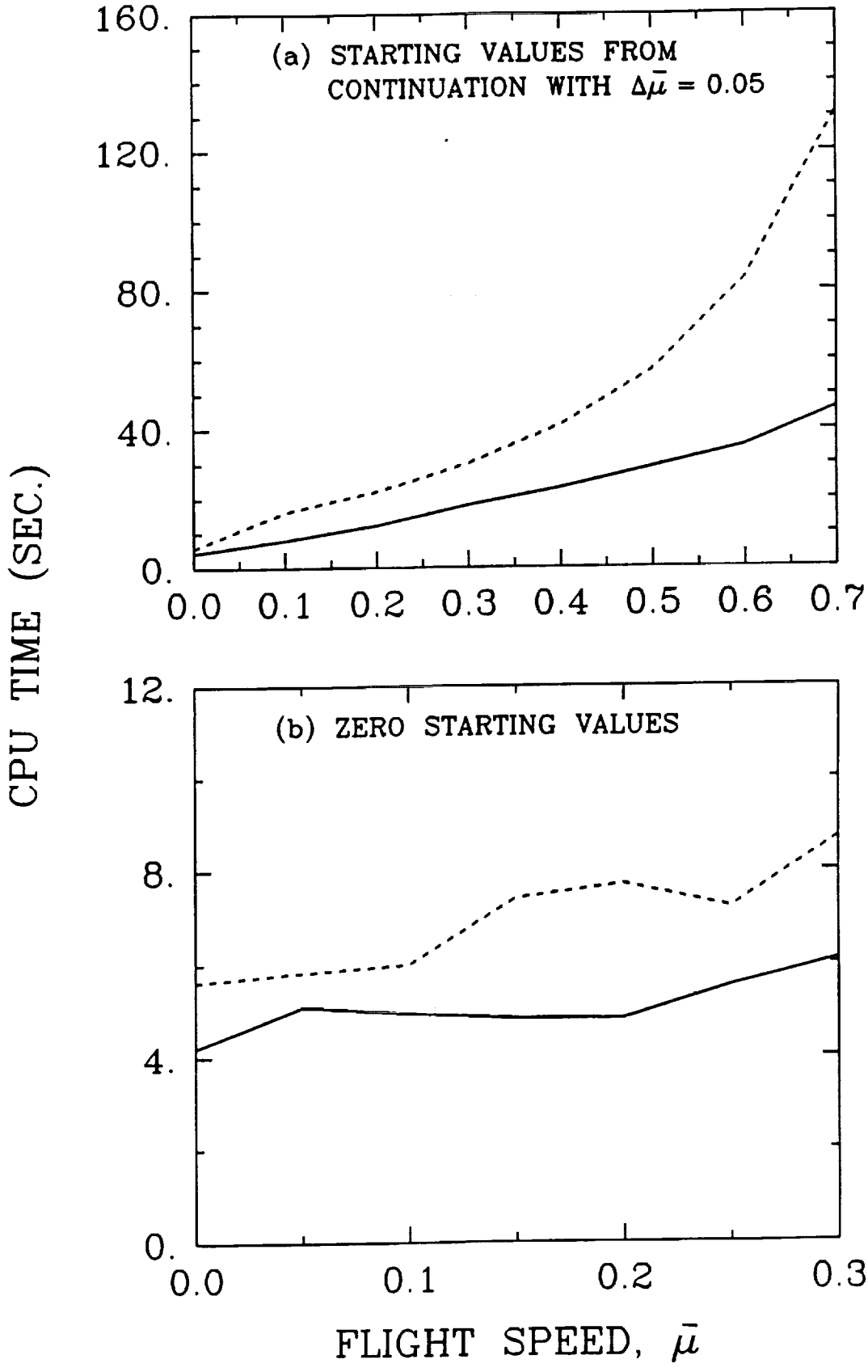

Fig. 4 Machine time comparison in the FEM-D with sequential and in-parallel schemes
(------- sequential, ——— in-parallel)

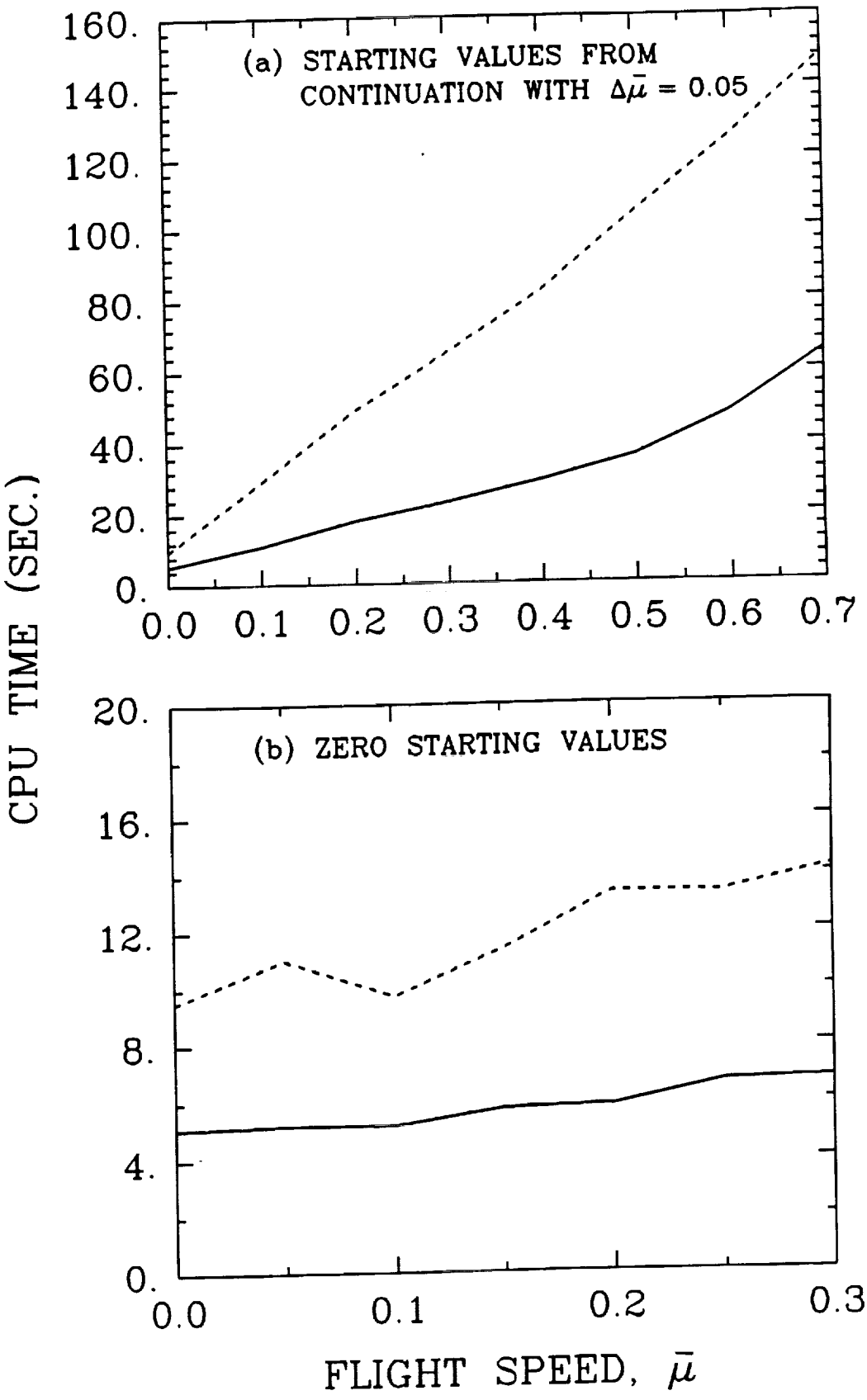

Fig. 5 Machine time comparison in the FEM-M with sequential and in-parallel schemes (------ sequential, —— in-parallel)

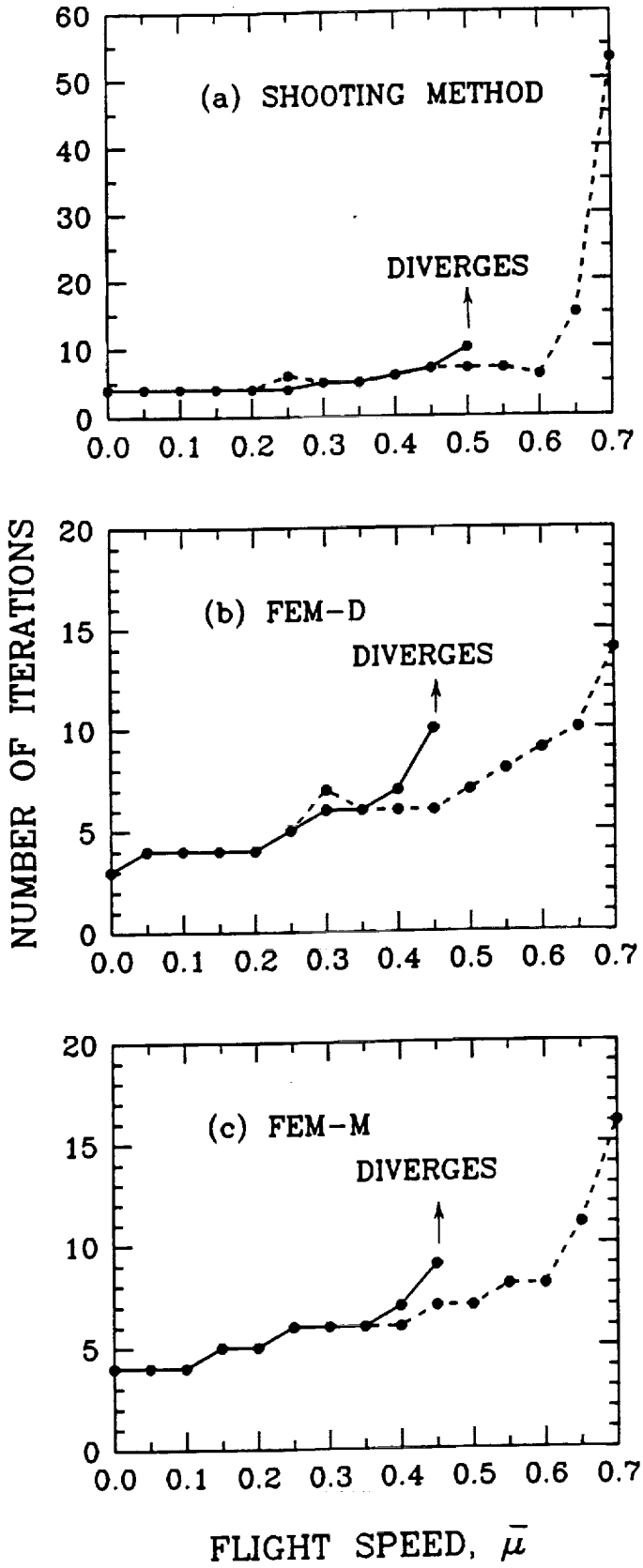

Fig. 6 Iteration counter comparison for the three trim analysis methods with zero sta-rting values
(——— without damping, ------- with damping)

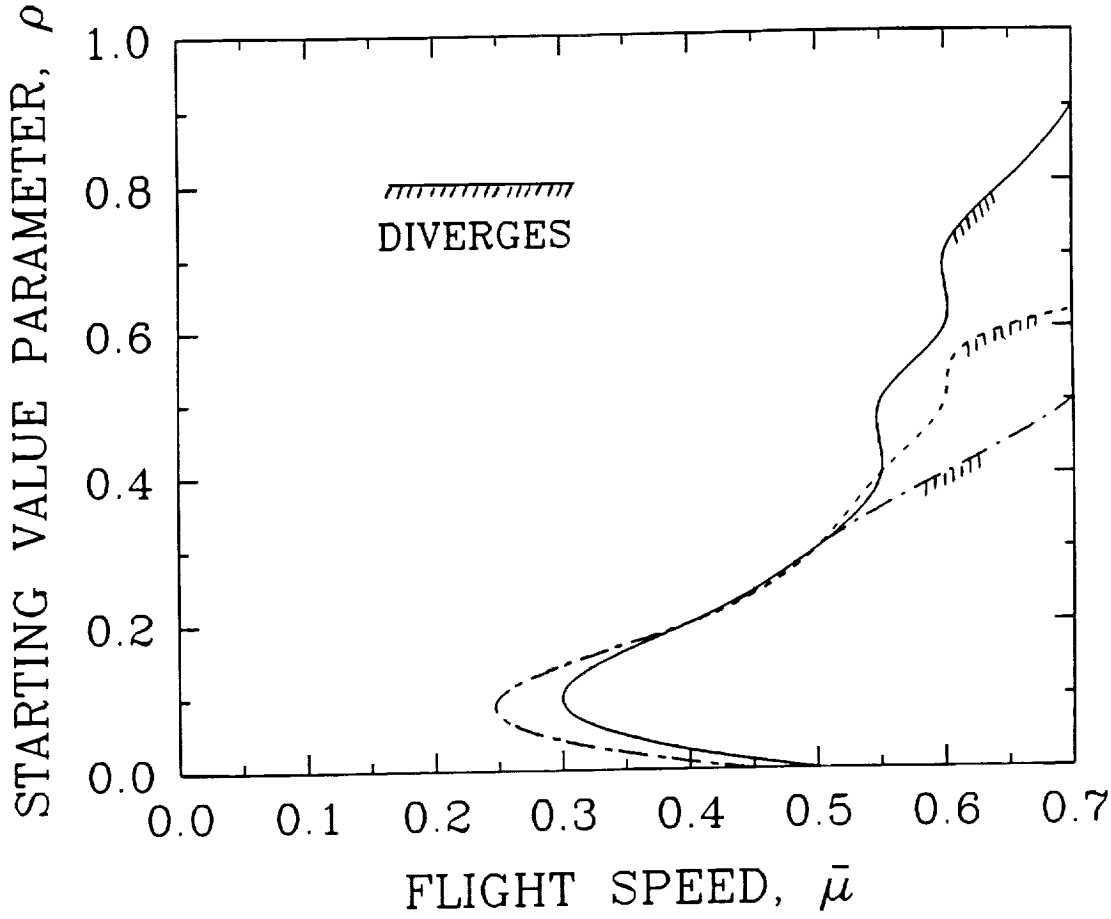

Fig. 7 Divergence boundary of the three trim an-
-alysis methods without damped Newton iteration
(—— Shooting ------ FEM-D -·-·- FEM-M; Converges
everywhere with damped Newton Iteration)

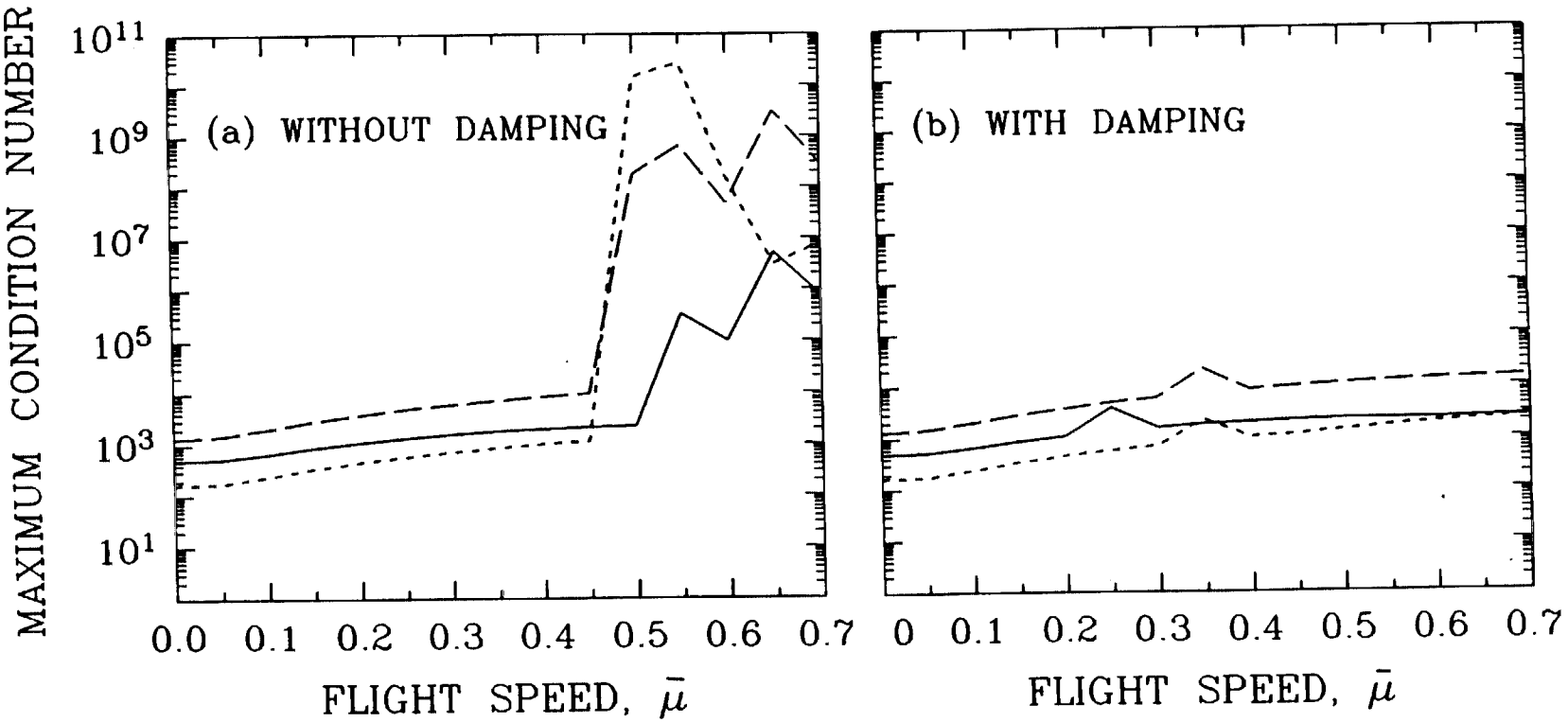

Fig. 8 Effects of damped Newton parameter on the Jacobian matrix condition number in the three trim analysis methods with zero st-
-arting values (—— Shooting, ----- FEM-D, ------- FEM-M)

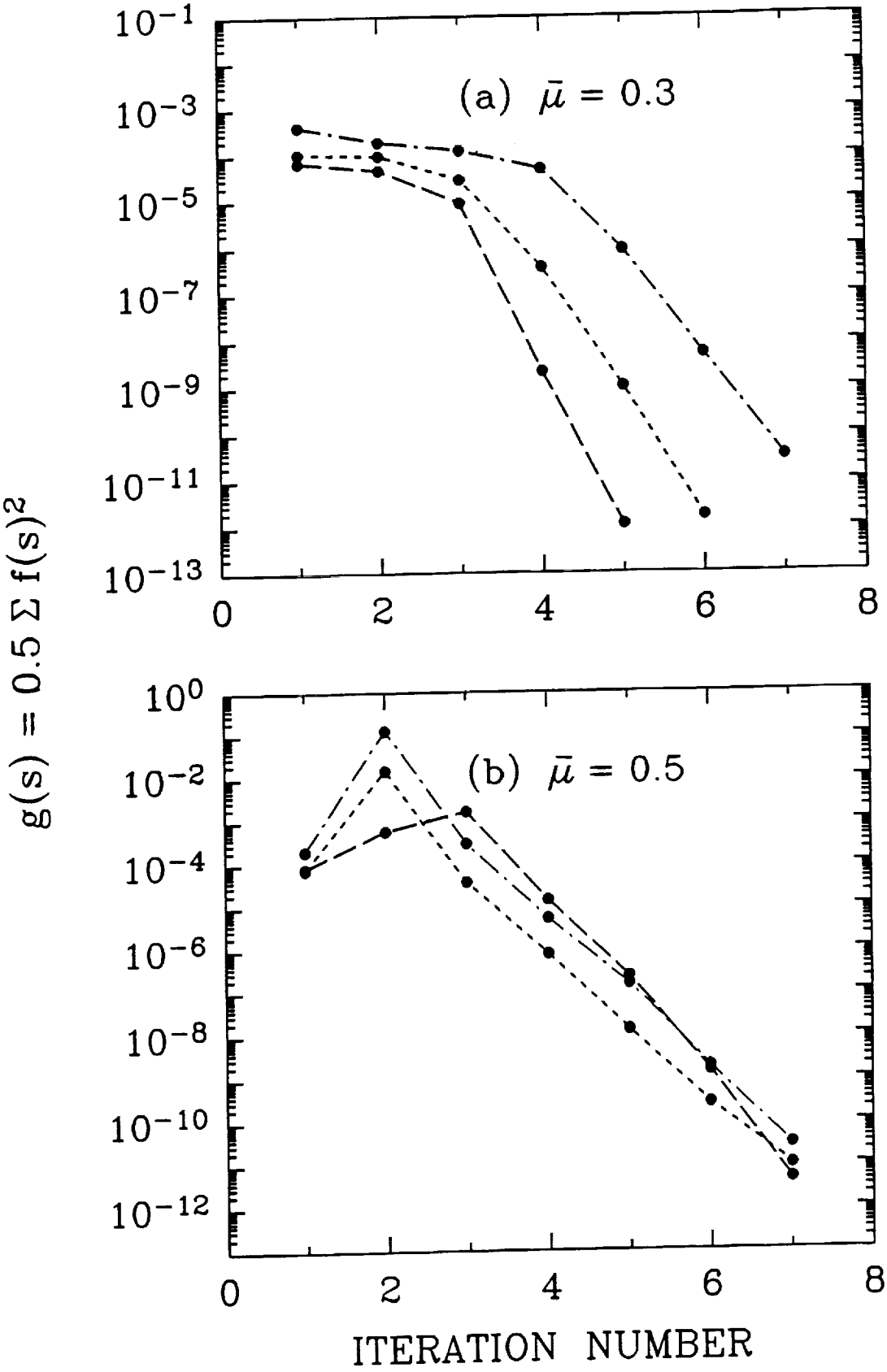

Fig. 9 Minimization of the objective function in the damped Newton iteration in the three trim analysis methods with zero starting values (---- shooting, -·-·- FEM-D, ------- FEM-M)

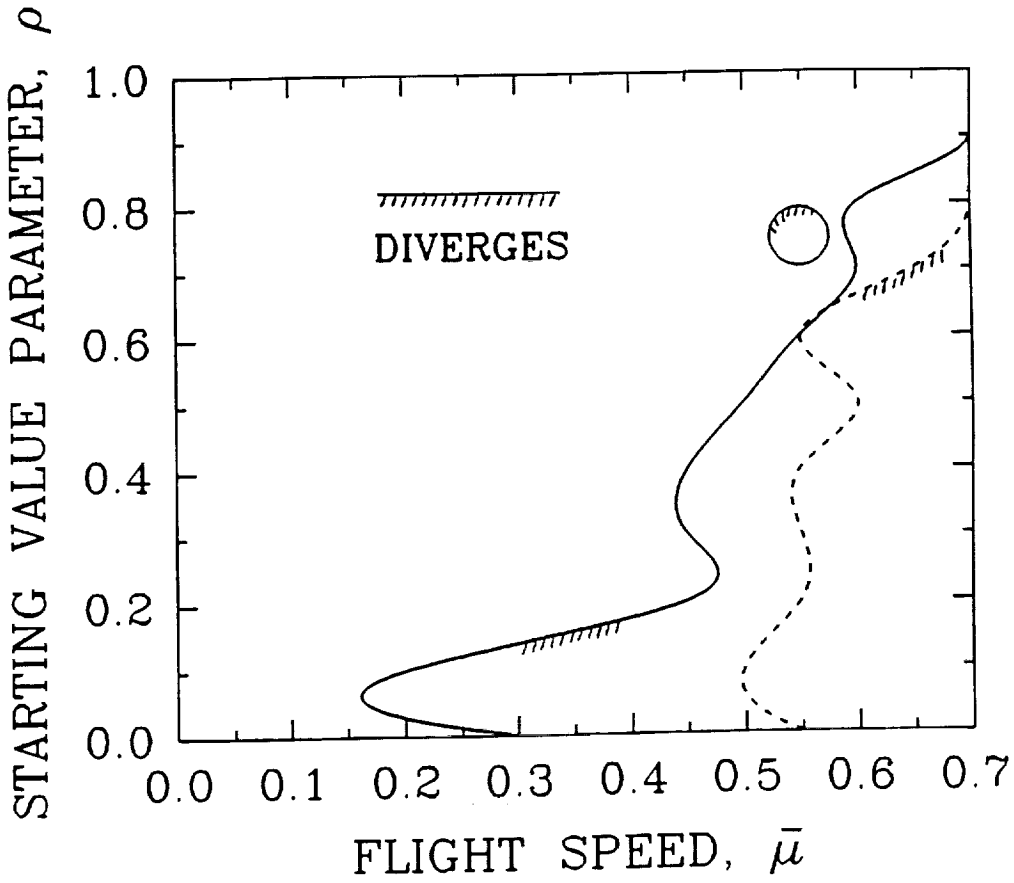

Fig. 10 Divergence boundary of the shooting method with sequential scheme (------- with damping, ——— without damping)

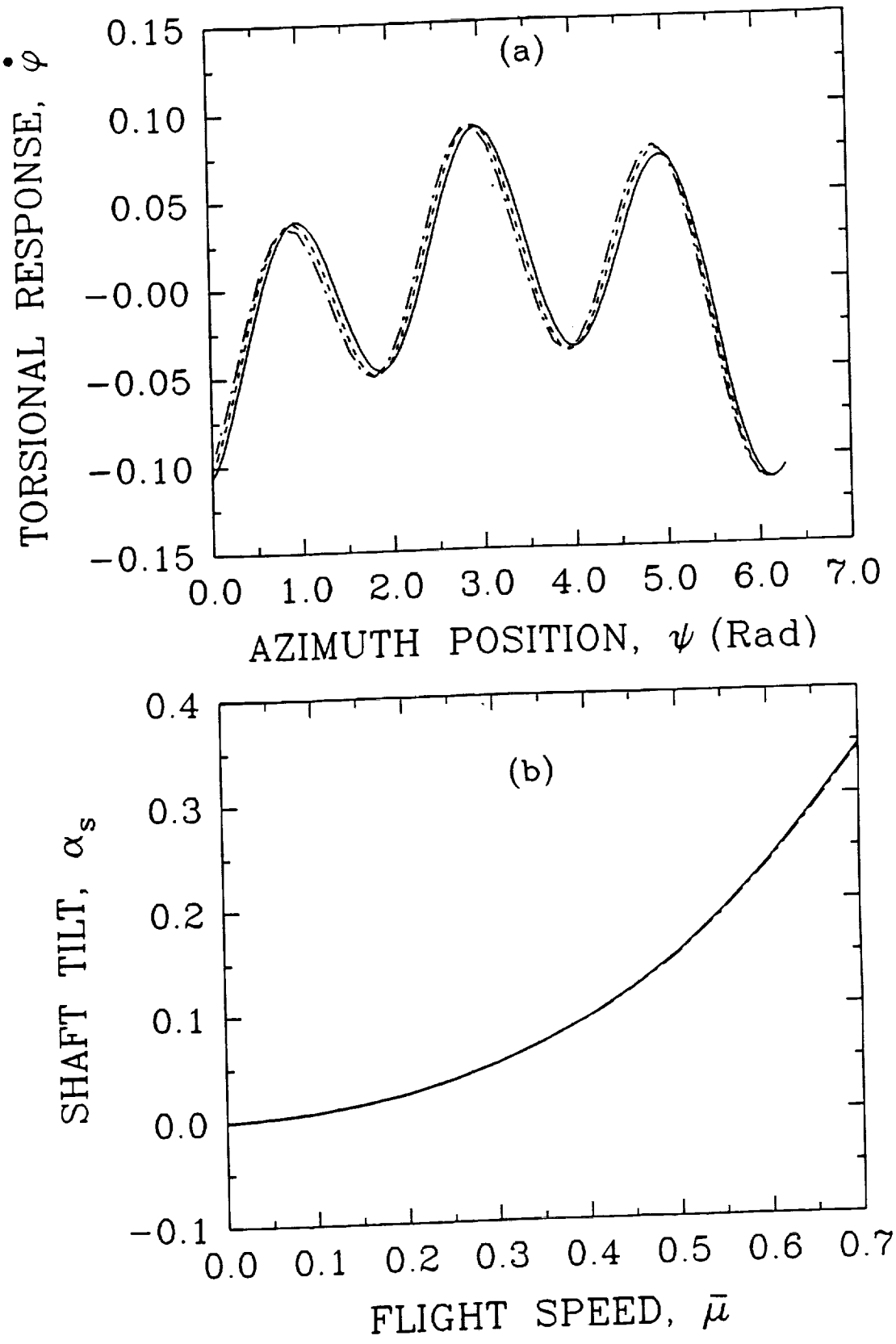

Fig. 11 Comparison of the torsional response and the shaft tilt angle from the three trim analysis methods (—— Shooting, ------ FEM−D, -·-·-· FEM−M)

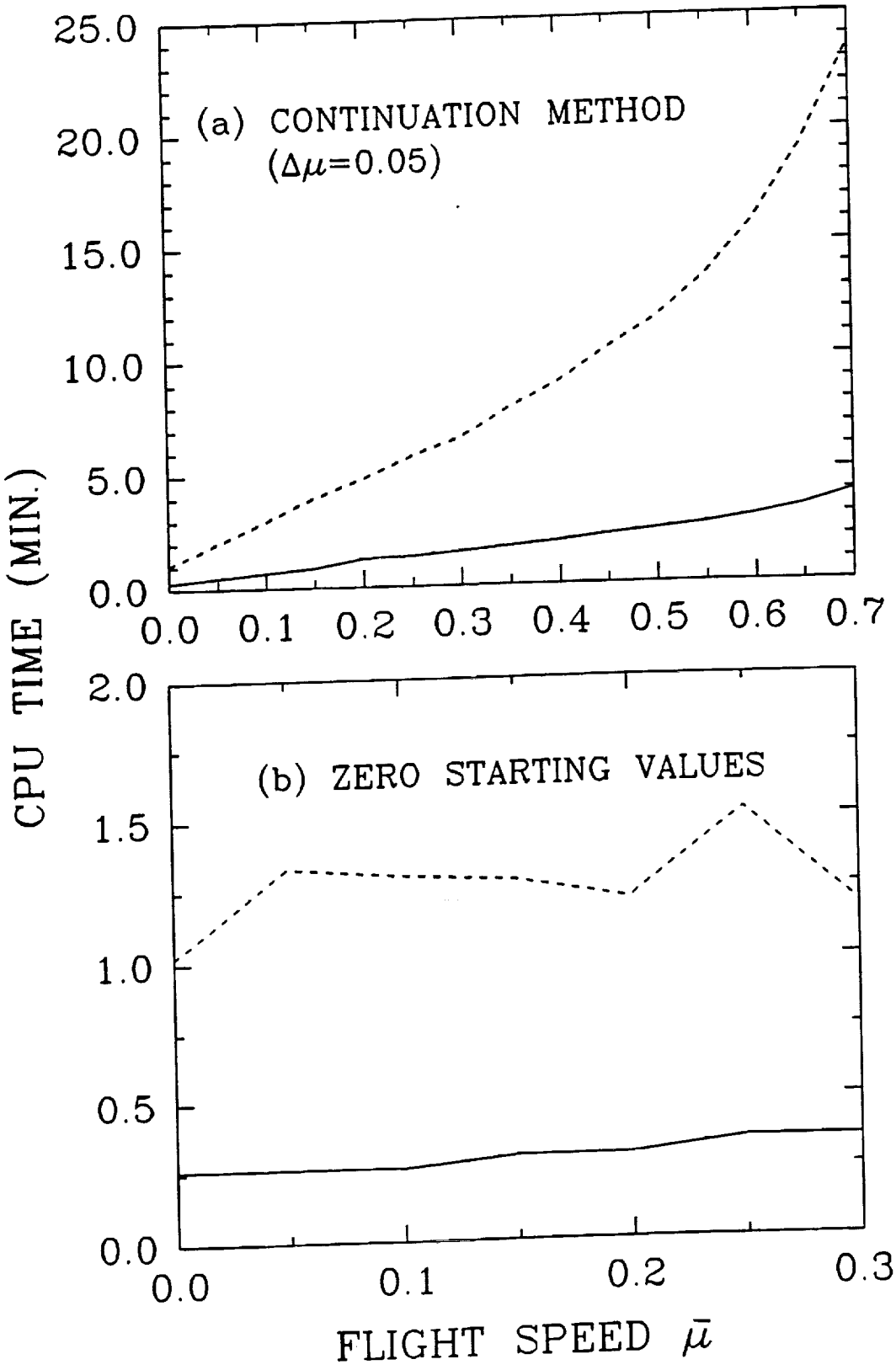

Fig. 12 Machine time comparison in the FEM-D with sequential and in-parallel schemes for flap-lag-torsion model (------ sequential, ——— in-parallel)

PART - II

FLOQUET EIGENANALYSIS

G. H. Gaonkar
N. S. Achar

An Exploratory Study of a Subspace Iteration Method as an Alternative to the QR Method for Floquet Eigenanalysis

Abstract

Floquet eigenanalysis requires a few dominant eigenvalues of the Floquet transition matrix (FTM). Although the QR method is used almost exclusively, it is expensive for such partial eigenanalysis; the operation counts and, thereby, the approximate machine time grow cubically with the matrix order. Accordingly, for Floquet eigenanalysis, the Arnoldi-Saad method, a subspace iteration method, is investigated as an alternative to the QR method. The two methods are compared for machine-time efficiency and computational reliability, which is quantified by the condition numbers of the required eigenvalues and the residual errors of the corresponding eigenpairs. The Arnoldi-Saad method takes much less machine time than the QR method with comparable computational reliability and offers promise for large-scale Floquet eigenanalysis (say, FTM order > 100).

Introduction

Floquet theory is the primary mathematical tool in the investigation of rotorcraft stability. Its application involves computation of the following: 1) the trim settings of initial state and control inputs for periodic response satisfying the flight conditions; 2) the FTM about that trim response, and 3) a few largest eigenvalues of the unsymmetric FTM, which often is a byproduct of the trim analysis. This study examines the computational aspects of the third item.

The information base on generating the FTM and its eigenanalysis is limited to relatively small-order systems (say, system or FTM order smaller than 100) and the generic QR

method is used almost exclusively for eigenanalysis (Ref. 1). Though the machine time needed to generate the FTM is sensitive to several factors, such as system nonlinearity, and defies generalization, it far exceeds the machine time for the eigenanalysis of the FTM. Therefore, for small-order systems, the search for a viable alternative to the QR method is not an issue. But for large-order systems, this search merits further investigation for two related reasons. First, the QR method is the recommended method for a complete eigenanalysis while Floquet eigenanalysis requires only a few most dominant eigenvalues or partial eigenanalysis. Second, for large systems, the QR method is expensive since the operation counts grow cubically with the matrix order (Refs. 2,3). Therefore, the machine time also grows approximately cubically with the matrix order. Further, the recent developments of the computer codes based on the Lanczos procedure for the partial eigenanalysis of large symmetric matrices (Ref. 2) motivated similar ongoing developments for the unsymmetric case.

There are two main approaches to this unsymmetric case: the simultaneous iteration methods (Refs. 4–7) and the Krylov subspace methods (Refs. 8–11). The success of the Lanczos procedures for the symmetric case (Ref. 2) has focused attention on the Krylov subspace methods, and it is also increasingly recognized that the simultaneous iteration methods are not competitive with the Krylov methods. The Krylov methods comprise two sub classes: methods based on orthogonal projection, such as the Arnoldi-Saad or AS method (Refs. 8,11), and those based on oblique projection, such as the Lanczos method (Ref. 9). Exploring the feasibility of these methods in the Floquet eigenanalysis, even within the limited scope of small-order FTMs, should prove useful if only to motivate further search for an alternative to the QR method for large rotorcraft systems. The present investigation chooses one of the Krylov subspace methods, the AS method, and compares it with the QR method for machine-time efficiency and computational reliability.

Arnoldi-Saad method

We begin with an n x n FTM, A. The AS method sequentially reduces A to an m x m upper Hessenberg matrix H_m (m << n), which contains the dominant eigenvalues of A. For extracting p dominant eigenpairs, the algorithm generates the Krylov subspace of dimension m > p. That is, the algorithm starts with an arbitrary vector v_1 and generates a sequence of vectors $v_1, v_2, \ldots, v_m$ by applying the Gram-Schmidt process to the sequence of vectors $\{v_1, Av_1, A^2v_1, \ldots, A^{m-1}v_1\}$ according to the recurrence formula (Ref. 8):

$$h_{j+1,j}\, v_{j+1} = Av_j - \sum_{i=1}^{j} h_{ij}\, v_i, \tag{1}$$

The h_{ij} (i = 1,..,j+1) are chosen so that v_{j+1} is orthonormal to v_i, i = 1,2,...,j and $\|v_{j+1}\| = 1$. Hence, the set of m vectors $\{v_1, v_2, \ldots, v_m\}$ forms an orthornormal basis for m-dimensional subspace spanned by $\{ v_1, Av_1, A^2v_1, \ldots, A^{m-1} v_1 \}$. It can be shown (Ref. 8) that the n x m matrix B, whose columns comprise m vectors $\{v_1, v_2, \ldots, v_m\}$, satisfies

$$H_m = B^t A B, \tag{2}$$

where H_m is an m x m upper Hessenberg matrix; B will be a tridiagonal matrix if A is symmetric. After generating H_m, its eigenpairs can be obtained using the QR method.

Convergence

In the AS method, the algorithm breaks down at the jth step (i.e., in the generation of the jth Krylov vector) if and only if $h_{j+1,j}$ in Eq. (1) becomes zero. But, $h_{j+1,j} = 0$ means that the Krylov vectors A^jv_1, $A^{j+1}v_1$ $A^{j+2}v_1, \ldots$, are linearly dependent on the previous j

Krylov vectors. The smallest value k of j at which the succeeding Krylov vectors become linearly dependent is known as the grade of the vector v_1 w.r.t. A (Ref. 12). For such a vector of grade k, there are constants $a_0, a_1,..,a_k$ such that

$$[a_0I + a_1A + a_2A^2 + a_3A^3 + ...+a_kA^k]\, v_1 = 0, \tag{3}$$

from which it follows that

$$[a_0 + a_1\lambda + a_2\lambda^2 + a_3\lambda^3 + ...+a_k\lambda^k] = 0, \tag{4}$$

where λ are the eigenvalues of A. Equation (4) is known as the minimal polynomial of v_1 with respect to A (Ref. 12). When Eq. (3) is satisfied, the vectors $v_1, v_2,...,v_k$ span the dominant subspace of dimension k of A, and the span of those vectors is invariant. Hence, the eigenvalues of $H_k = B^tAB$ are the exact dominant eigenvalues of A.

On the other hand, when the number of Krylov vectors chosen is less than the grade of the vector v_1, the accuracy of the eigenvalues computed decreases with their decreasing order of magnitude; the most dominant eigenvalue will be the most accurate and the smallest eigenvalue will be the least accurate. However, it must be mentioned that issues such as roundoff errors and reorthogonalization (Ref. 8) are not addressed in this exploratory study.

Eigenvalue reliability

We use two eigenvalue reliability parameters: condition number of an eigenvalue and residual error of an eigenpair (eigenvalue and corresponding eigenvector). The matrix A and its transpose A^t have the same eigenvalues. We assume that λ is one such simple

eigenvalue (of multiplicity one) and that $\mathbf{x}$ and $\mathbf{y}$ are the corresponding right and left eigenvectors; that is,

$$A\mathbf{x} = \lambda\mathbf{x} \text{ and } A^t\mathbf{y} = \lambda\mathbf{y} \tag{5}$$

Then the condition number of λ is given by (Ref. 12)

$$\text{cond}(\lambda) = |\mathbf{y}^t\mathbf{x}|^{-1} \tag{6}$$

We emphasize that λ is usually complex, as are the eigenvectors. It is $\mathbf{y}^t$ (not the hermitian transpose of $\mathbf{y}$) that is used. Further, the vectors are normalized, that is, $\|\mathbf{x}\| = \|\mathbf{x}^h\ \mathbf{x}\| = 1 = \|\mathbf{y}\| = \|\mathbf{y}^h\ \mathbf{y}\|$. If A is hermitian, $\|\mathbf{y}^t\ \mathbf{x}\| = 1$. The significance of cond(λ) is demonstrated by the following relation:

$$|\delta\lambda| < \|\delta A\| \text{ cond } (\lambda), \tag{7}$$

where $\|\delta A\|$ represents the spectral norm of the matrix of perturbations of the FTM due to sources such as roundoff and discretization. Further, $\delta\lambda$ represents the resulting perturbation of λ due to working with the computed $A + \delta A$, instead of A. In other words, the computed eigenvalue is $\lambda + \delta\lambda$, which is the exact eigenvalue of $A + \delta A$. Thus, cond(λ) provides a measure of the sensitivity of an eigenvalue, typified by $\delta\lambda$. If small changes in the elements of the FTM can lead to arbitrarily large changes in an eigenvalue, then the eigenvalue problem for that eigenvalue is said to be ill-conditioned. That a matrix is well-conditioned for eigenvalue computations is no guarantee that it is well-conditioned for eigenvector computations. Though the condition number approach has a rigorous basis, a similar approach for eigenvectors is too involved for computing the error bounds.

Therefore, we study the reliability of the computed eigenpair (λ,$\mathbf{x}$) by the residual error approach, which gives the relative error measure ϵ. That is,

$$\epsilon = \frac{\|\mathbf{A}\mathbf{x}-\lambda\mathbf{x}\|}{\|\lambda\mathbf{x}\|} = \frac{\| \mathbf{r} \|}{\| \lambda \|}, \tag{8}$$

where $\|\mathbf{r}\|$ is the Euclidean norm of the residual error. It appears that cond(λ) and ϵ should provide adequate information on the reliability of a computed eigenpair.

Results

The eigenanalysis comprises computation of a few dominant eigenvalues, including their eigenvectors and the corresponding condition numbers and residual errors; see Eqs. (7) and (8). These computations from the AS method are compared with those from the QR method for FTMs of various order. Table 1 is a representative example.

The QR results in the last row of Table 1 are taken to be exact; very low residual error and condition number are noteworthy. Before comparing the results from these two eigenanalysis methods, it is important to realize that the eigenanalysis of large unsymmetric matrices represents a computational barrier and several issues concerning the minimum dimension of a subspace matrix merit further research. Nevertheless, comparison with the QR results shows that the damping and frequency results from the 20 x 20 subspace matrix are accurate up to six and two significant figures, respectively, with comparable condition numbers, and that the accuracy increases with the increasing dimension of the subspace matrix. For the AS method, two points are emphasized. First, the accuracy is independently corroborated by the respective residual error results. Second, the order of magnitude of the eigenvalue condition number is close to the ideal value of

one, which demonstrates that the eigenvalue computations are well conditioned. The most distinguishing feature is the relative saving in machine time, which is shown in Fig. 1; 53.4 versus 19.8 seconds for a subspace dimension of 20 x 20. This trend offers great promise for large-order FTMs. Because the machine time required for the QR method increases almost cubically with the order of the FTM, the relative saving increases rapidly with the increasing order.

Concluding remarks

For the partial eigenanalyis of the FTM, the AS and the QR methods are compared for machine-time efficiency and computational reliability. The numerical experiment shows that the Arnoldi-Saad method is more economical than the QR method with comparable computational reliability. The partial eigenanalysis of large-order FTMs is important to comprehensive stability analysis of rotorcraft, and relatively little is known. Given this fact, the results should serve as a useful reference point.

References

1. Gaonkar, G.H., and Peters, D.A., "Review of Floquet Theory in Stability and Response Analysis of Dynamic Systems with Periodic Coefficients," The R. Bisplinghoff Memorial Symposium Volume on Recent Trends in Aeroelasticity, Structures and Structural Dynamics, University Presses of Florida, 1987, pp. 890-897.
2. Cullum, J.K., and Willoughby, R.A., *Lanczos Algorithms for Large Symmetric Eigenvalue Computations*, Vol. 1 (Theory) and Vol. 2 (Programs), Birkhause, Boston, 1985.

3. Ravichandran, S., Gaonkar, G.H., Nagabhushanam, J. and Reddy T.S.R., "A Study of Symbolic Processing and Computational Aspects in Helicopter Dynamics," *Journal of Sound and Vibration*, Vol. 137, (3), March 1990.

4. Stewart, W.J. and Jennings, A., "A Simultaneous Iteration Algorithm for Real Matrices," ACM *Transactions for Mathematical Software*, Vol. 7, No. 2, June 1981, pp. 184-198.

5. Stewart, W.J., and Jennings, A., "Simultaneous Iteration for Computing Invariant Subspaces of Non-Hermitian Matrices," *Nurmerische Mathematik*, Vol. 25, pp. 123-136.

6. Jennings, A., *Matrix Computation for Engineers and Scientists*, John Wiley, 1977, Chapter 10.

7. Stewart, G.W., "SRRIT-A FORTRAN Subroutine to Calculate the Dominant Invariant Subspace of a real Matrix," Technical Report TR-514, Computer Science Department, University of Maryland, 1978.

8. Saad, Y., "Variations in Arnoldi's Method for Computing Eigenelements of Large Unsymmetric Matrices," *Linear Algebra and Its Applications*, Vol., 34, 1980, pp. 269-295.

9. Parlett, B.N., Taylor, D.R. and Liu, Z.A., "A Look-ahead Lanczos Algorithm for Unsymmetric Matrices," *Linear Algebra Applications*, Vol. 34, 1985, pp. 105-124.

10. Kahn, W., Parlett, B.N., and Jiang, E., "Residual Bounds on Approximate Eigensystems of Nonnormal Matrices," SIAM *Journal of Numerical Analysis*, Vol. 19, 1982, pp. 470-484.

11. Cullum, Jane and Willoughby, R.A., "Practical Procedure for Computing Eigenvalues of Large Sparse Nonsymmetric Matrices," Large Scale Eigenvalue Problems, North Holland, Mathematics Studies, Vol. 127, New York, 1986, pp. 193-240.

12. Wilkinson, J.H., *The Algebraic Eigenvalue Problem*, Clarendon Press, New York, 1965.

SUBSPACE DIMENSION	DAMPING LEVEL	NONUNIQUE FREQUENCY	CPU TIME (SEC.)	RESIDUAL ERROR	EIGEN-VALUE CONDITION NUMBER
12 (AS)	-0.104757	0.658677E-2	13.50	0.24E-01	1.8
16 (AS)	-0.105274	0.456415E-2	16.08	0.21E-02	1.9
20 (AS)	-0.105322	0.428022E-2	19.76	0.23E-04	2.0
24 (AS)	-0.105322	0.429649E-2	23.92	0.30E-06	2.4
92 (QR)	-0.105322	0.429647E-2	53.40	0.29E-15	3.4

Table 1 Machine time and computational reliability results for the Arnoldi-Saad method vis-a-vis QR method (FTM dimension = 92x92)

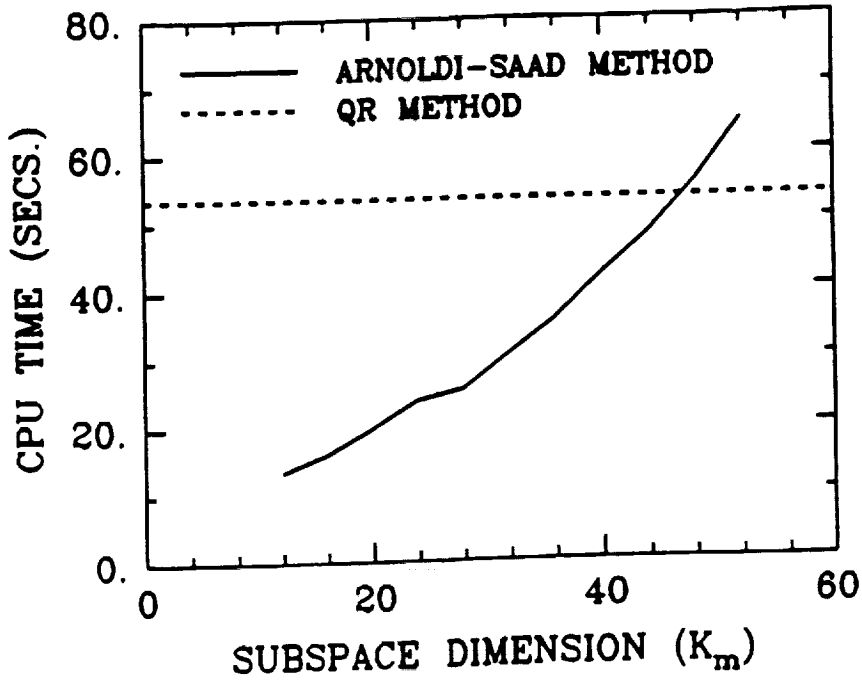

Fig. 1 Comparison of machine times required by the Arnoldi-Saad and the QR methods (FTM dimension = 92x92)